Exact distribution of the quantal content in synaptic transmission

Krishna Rijal[a], Nicolas I.C. Müller[b], Eckhard Friauf[b], Abhyudai Singh[c], Ashok Prasad[d,1], and Dibyendu Das[a,1]

[a]Department of Physics, Indian Institute of Technology Bombay, Powai, Mumbai 400076, India
[b]Animal Physiology Group, Department of Biology, University of Kaiserslautern, Kaiserslautern, Germany
[c]Departments of Electrical and Computer Engineering, Biomedical Engineering and Mathematical Sciences, University of Delaware, Newark, DE 19716, USA
[d]Department of Chemical and Biological Engineering, Colorado State University, Fort Collins, Colorado, USA
[1]To whom correspondence should be addressed: dibyendu@phy.iitb.ac.in; ashok.prasad@colostate.edu

April 18, 2023

Abstract

The transfer of electro-chemical signals from the pre-synaptic to the post-synaptic terminal of a neuronal or neuro-muscular synapse is the basic building block of neuronal communication. When triggered by an action potential, the pre-synaptic terminal releases neurotransmitters into the synaptic cleft through exocytotic vesicle fusion. The number of synaptic vesicles that fuse, i.e., the quantal content, is stochastic, and widely assumed to be binomially distributed. However, the quantal content depends on the number of release-ready vesicles, a random variable that depends upon a stochastic replenishment process, as well as stochastic interspike intervals of action potentials. The quantal content distribution suitably accounting for these two stochastic processes was not known explicitly in the literature. Here we analytically obtain the exact probability distribution of the number of vesicles released into the synaptic cleft, in the steady state reached during stimulation by a train of action potentials. We show that this distribution is binomial, with modified parameters, only when stimulated by constant frequency signals. Other forms of stochastic stimulation, e.g. Poissonian action potential train, lead to distributions that are non-binomial. The general formula valid for arbitrary distributions of the input inter-spike interval may be employed to study neuronal transmission under diverse experimental conditions. We provide exact theoretical moments which may be compared with experiments to estimate the model parameters. We corroborate our theoretical predictions through comparison with the quantal content distributions obtained from electrophysiological recordings from MNTB-LSO synapses of juvenile mice. We also confirm our theoretically predicted frequency dependence of mean quantal content by comparing with experimental data from hippocampal and auditory neurons.

Author summary

The synapse is a specialized junction between a pre-synaptic neuron and another neuron or muscle cell for neuronal communication. Action Potentials (APs) in the

pre-synaptic neuron reach the synapse and trigger neurotransmitter-loaded vesicles to release their cargo in the nanometer-sized gap between the two cells. The pool of vesicles that are ready to be released is then replenished. The number of vesicles that release neurotransmitters, the quantal content and the number that are replenished are both random numbers. However, the probability distribution that describes the quantal content while taking the stochastic replenishment process into account was not known analytically, although a binomial distribution was often assumed. Exact mathematical results are not frequent in biological processes, but we could find an exact analytical solution of the problem in the long time (steady state) limit of AP stimulation. We show that for constant frequency stimulation the distribution of quantal content is indeed a binomial, but for stochastic stimulations (like Poisson train) generically it is not a binomial. The exact distributions and moments that we derive would greatly simplify estimation of model parameters, as we demonstrate by comparing our theory with data from electrophysiological recordings of auditory neurons.

Introduction

The human brain is arguably the most complex natural object in the known universe. Its complexity, as well as its capabilities, are a product of its roughly 86 billion [1] neurons that make approximately 10^{15} connections [2] with each other. The majority of these connections are chemical synapses, where a pre-synaptic neuron communicates with a post-synaptic neuron through neurotransmitter release in a few nm thick synaptic cleft (Fig 1a). Neurotransmitter release takes place by the fusion of neurotransmitter-containing lipid vesicles with the pre-synaptic plasma membrane at the synaptic cleft, thereby releasing their cargo into the synaptic cleft (Fig 1a). Synaptic vesicle (SV) fusion is controlled by calcium dynamics and is initiated by an action potential (AP) in the pre-synaptic neuron. Neurotransmitter release may cause either an excitatory or inhibitory signal at the post-synaptic site, that could result in an AP or the suppression of one [3]. Thus, SV release from pre-synaptic

terminals is a fundamental feature of all information processing in the nervous system.

Decades of study since Castillo and Katz [4] first proposed the quantal theory of neurotransmitter release have revealed the basic characteristics of the process. The swelling or bouton in the pre-synaptic neuron that constitutes the pre-synaptic terminal contains vesicle-rich active zones (AZ) proximal to the plasma membrane. The AZ regions are surrounded by a larger vesicle-rich area, as well as mitochondria that supply energy and help regulate calcium dynamics, and dense actin filaments involved in vesicle transport and recycling [5,6]. Detailed micro-structural and electrophysiological studies have led to a consensus on a vesicle pool model of neurotransmitter release at a descriptive level [6–8]. According to this model, SVs can be divided into two or three pools. The smallest pool is the readily-releasable pool (RRP) situated in the AZ, that is partially released immediately after stimulation. The remaining pools are the Recycling pool (RP) and the Resting pool [7] (also named reserve pool in [6]). The pool sizes vary widely between types of neurons and species, and also within individual boutons of a single neuron [7]. Arrival of an AP at the pre-synaptic terminal leads to fusion of vesicles from the RRP with the plasma membrane and release of the neurotransmitter cargo into the synaptic cleft. As the RRP is depleted, vesicles from the RP are mobilized to replenish the docking sites in the AZ, and vesicle recycling also kicks in. With continual stimulation the vesicles from the Resting pool may get mobilized, however this depends upon the type of neuron. In human hippocampal neurons, for example, the Resting pool seems to be rarely activated [6].

Thus, SV fusion in most neurons is well described by a two-pool model (Fig 1a) and a two-step process. Initially, each AP releases a fraction of the docked vesicles constituting the RRP, leading to a decline in the average number of vesicles released over time. With sustained stimulation, the RRP starts to be replenished from the recycling pool and ultimately, a balance between SV fusion and replenishment leads to the development of a steady state, as long as the rate of stimulus does not exceed the maximum capacity for replenishment [7,9]. The SV replenishment and fusion processes are intrinsically stochastic. As a result, the neurotransmitter release is also

stochastic and is one of the important sources of noise in the nervous system [10]. The stochasticity in SV release affects the information transfer from a pre-synaptic neuron to a postsynaptic neuron, and it has been argued that it may sometimes enhance information processing at synapses [11,12].

Though much of the earlier analysis on theoretical modeling of synaptic transmission was carried out assuming a deterministic process [13–15], there is a significant literature studying the process using a probabilistic approach [16–22]. Empirical observations had shown that the binomial distribution was a good fit to the statistics of quantal release as far back as 1975, and this has been the basis of the majority of fluctuation analysis [12,16,20,22–27]. Limitations of the binomial assumption due to biological complexities were recognized (reviewed in Ref. [8]). But it has generally been assumed that the basic model of neurotransmitter release follows a binomial distribution for the number of released vesicles b (here called quantal content) [12,20–22,28–30], namely $B(n_-, p_r, b) = \binom{n_-}{b} p_r^b (1-p_r)^{n_- - b}$, where probability of release is p_r. Since the replenishment process is itself stochastic, the number of docked vesicles n_- just prior to a burst is random. Consequently, the resultant form of the quantal content distribution remains unknown. Approximate theories in the literature continued to assume this to be binomial, often replacing n_- by its mean value $\langle n_- \rangle$ [20–22,28,29,31,32]. In this paper we consider the stochastic evolution of the number of docked vesicles $n(t)$ due to the stochastic replenishment process during time t between two APs, as well as possible randomness in the interspike intervals (ISIs) $t = t_s$. This leads to a stochastic $n_- = n(t_s)$ just prior to the arrival of an AP. Exact analytical results, based on this stochastic treatment, are obtained for the distribution of the quantal content.

For a specific time history of stimulation by APs, and a given set of model parameters, a systematic formalism treating the docked vesicle number stochastically, was developed in a set of works [33–36]. Exact relationships between probability of successive postsynaptic currents after every AP, were formally written down, assuming a parameter set for the model. The expressions involved multiple nested summations [34] which could not be handled analytically. Using Bayesian inference

or maximum-likelihood principle [33,34,36], the authors estimated the model parameters. The calculations involved variety of computational techniques like Expectation-Maximization algorithm [33], Metropolis-Hastings sampling method [34], and Nested Particle Filter algorithm [36]. In this work, we start with exact recursive relations between probabilities of the docked vesicle numbers after every AP spike, in similar spirit as [33,34]. But then we move on further to show that in the *long time limit*, the distribution of quantal content becomes *analytically tractable*. We can thus derive exact formulae that describe the probability distribution as well as its moments under these conditions.

For a synaptic system (Fig 1a) with a finite maximal number M of docked vesicles, sustained stimulation by APs for long enough time typically leads to a *steady state* [7,12,20,37,38]. In such a steady state, the time-varying calcium concentration-dependent replenishment rate k_t and release probability p_{rt} would saturate to constant values $k = k_\infty$ and $p_r = p_{r\infty}$ (see representative curves in Section 8 of supplementary information (SI) following a model of Ref. [15]). The quantal content distribution, which is the main quantity of our interest, also reaches a time-independent form in this limit. In the steady state, we prove that for commonly used constant ISIs, the distribution of quantal content b is indeed a binomial $B(M, p_{rb}, b)$ (where p_{rb} is a function of p_r, k, and the frequency of stimulation). However, for a Poisson input stimulation with exponentially distributed ISIs, the quantal content distribution is non-binomial and we obtain its exact closed form. Apart from these special cases, for any general stochastic stimulation with uncorrelated ISIs (t_s) drawn from a distribution $g(t_s)$ (see Fig 1b), we obtain a formal solution for the quantal content distribution, in the steady state.

In practice, there may be systems where steady state is hard to reach due to long relaxation times, or complex temporal dynamics of synaptic plasticity, or the nature of stimulation. In such cases, the treatment of [33,34,36] are helpful. However, experimentalists have used deterministic stimulation as well as Poisson trains and even claimed that Poisson stimulations yield better parameter estimates [39]. Stochastic stimulations with ISIs drawn from other distributions ($g(t_s)$) can also be easily de-

signed and implemented experimentally to test our predictions. Input stimulations *in vivo* are also expected to be stochastic [40,41]. Thus, there are contexts where the treatment of stochastic stimulations analyzed in this paper may be naturally useful. In such situations model parameters may be estimated by direct matching of exact theoretical moments of the quantal content (obtained in this paper) with those obtained experimentally. Exact closed form results significantly reduce if not eliminate computational cost, unlike earlier works. Furthermore, closed form results are useful for subsequent theoretical development.

We do not explicitly consider the process of vesicle priming [42] separately and assume that all processes including transport and priming that prepares vesicles for fusion can be incorporated through the rate k (Fig 1a). We also do not consider processes in the post-synaptic terminal after neurotransmitter release, such as post-synaptic receptors saturation or desensitization. Finally, we consider the distribution of the quantal size to be narrow, such that the postsynaptic current may be assumed proportional to the quantal content. Since the analytical tractability was the main emphasis, we work with the minimal model which most earlier works in the literature have used, keeping aside the above mentioned complexities for future inquiries.

Results

A stochastic model of vesicle release triggered by action potentials

A schematic diagram of a chemical synapse is shown in Fig 1a, with the vesicle-rich pre-synaptic terminal on the left and the post-synaptic terminal with neurotransmitter receptors on the right. The cartoon shows only a few vesicles but the actual number in the pre-synaptic terminal can vary broadly [33,43,44]. In the pre-synaptic terminal, SVs packed with neurotransmitters attach to docking sites. The arrival of an AP triggers the stochastic fusion of a few SVs with the pre-synaptic membrane followed by neurotransmitter release. We assume that there is a maximum number

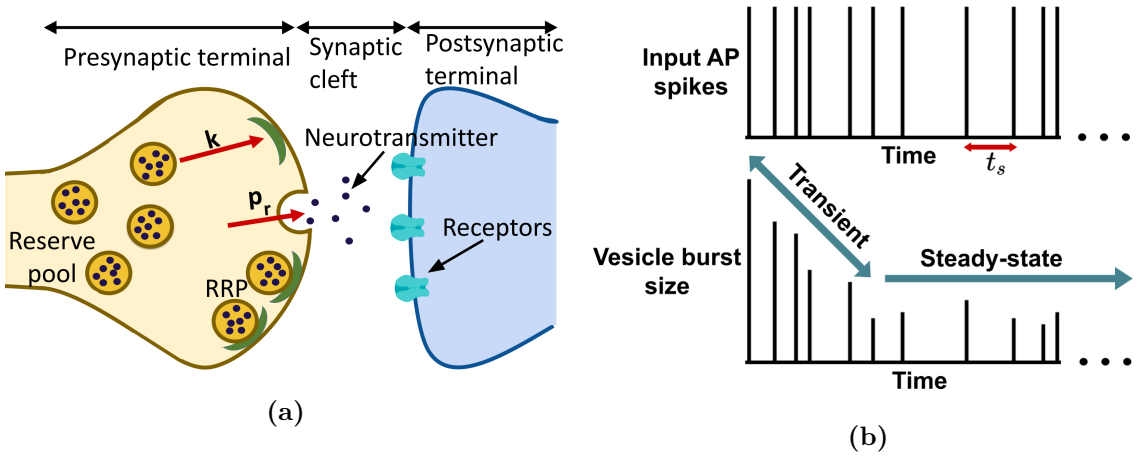

Fig 1: A schematic of the synapse and synaptic communication data. (a) Schematic picture of a chemical synapse. On the left is the pre-synaptic terminal or bouton and on the right is the post-synaptic terminal, with the synaptic cleft in between. The pre-synaptic terminal contains a pool of docked vesicles (RRP) and another reserve pool of vesicles that can occupy empty docked sites after vesicle fusion. The rate of docking k and the fusion and release probability p_r of vesicles are shown. The post-synaptic terminal has receptors for the neurotransmitters released from the fused vesicles. (b) Synaptic communication. The illustration shows an input spike train with random intervals t_s, and the output quantal content with initial transient and eventual steady-state regions.

M of available docking sites, and that docking sites are refilled from the vesicle pool at a rate proportional to the number of empty sites, i.e., a rate equal to $k(M-n)$, where n is the number of already docked vesicles and k is the docking rate per empty site [20,22]. We assume that docked vesicles may be released probabilistically after an AP but do not otherwise detach. We consider experimentally relevant scenarios (like in Ref. [38]) where a train of APs arrive at the pre-synaptic neuron. In this study we consider the general possibility that the time intervals t_s between two consecutive spikes of the input AP may be random but uncorrelated, following a distribution $g(t_s)$. Experimentally often fixed frequency oscillatory input AP are used with constant $t_s = T$ [20,21,30,38], which would correspond to $g(t_s) = \delta(t_s - T)$. The number b of SVs that fuse and release neurotransmitters after the arrival of an AP is a stochastic variable, referred to as the quantal content. Following [12,20,21,28,30],

we assume that the quantal content b after an AP follows a binomial distribution $B(n_-, p_r, b) = \binom{n_-}{b} p_r^b (1-p_r)^{n_- - b}$, where p_r is the probability of release (in the steady state) and n_- is the instantaneously docked vesicle number before the AP arrives.

We note that the quantal content b is stochastic not just because it is binomially distributed, but because the number of docked vesicles n_- which form its source is itself stochastic. As we discussed above, the ready to release docked vesicle number n grows stochastically with time, and at random intervals t_s when an AP appears, $n = n_-$ suddenly become $n = n_- - b$. Thus in the steady state, the exact distribution of b may be obtained by averaging the binomial over the stochastic n_-, which leads to a revised distribution as we would see below.

The quantal content distribution $Q^{ss}(b)$ in the steady state

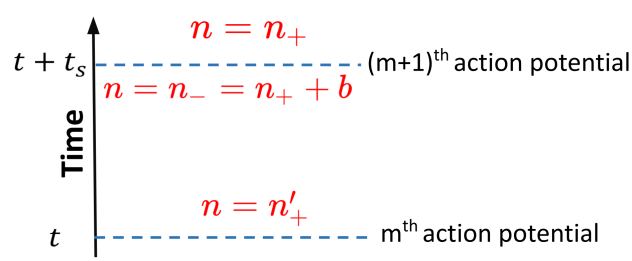

Fig 2: Model variables. Schematic showing the variables we used to describe the time evolution of the number n of the vesicles inside the pre-synaptic neuron, from the value n'_+ after an action potential to n_- just prior to the next action potential after time t_s and then its sudden reduction to n_+ after a burst of size b.

In Fig 2, the number variation of vesicles in the pre-synaptic neuron is shown schematically. Starting with $n = n'_+$ after an AP, the number grows to $n = n_- = n_+ + b$ in time t_s, at which the appearance of the next AP leads to the fusion of b vesicles, resulting in a sudden decrease of n from $n_+ + b$ to n_+. Before the arrival of APs in the pre-synaptic terminal, the instantaneous number of docked vesicles n_- may be assumed to be at its maximum value, M, and the quantal content b is thus expected to be the largest. With the continuation of the stimulus, the average number of n_- gradually decreases to a steady-state level given by a balance between

the vesicle release and replenishment process. In this long-time steady-state limit, our goal is to obtain an explicit expression for the size distribution $Q^{ss}(b)$ of b, summing over the likelihood of stochastic vesicle number n_-, as follows:

$$Q^{ss}(b) = \sum_{n_-=0}^{M} B(n_-, p_r, b) P_-^{ss}(n_-). \tag{1}$$

To calculate $Q^{ss}(b)$, we need to first obtain $P_-^{ss}(n_-)$, the steady-state probability distribution of having $n = n_-$ docked vesicles just before an AP. As mentioned previously, n_- and hence $P_-^{ss}(n_-)$ is regulated by the random processes of growth of n and the appearance of AP at a random t_s. To study the growth of n, we introduce the time-dependent conditional probability $p(n, t|n'_+)$, of having n number of docked vesicles at time t, given n'_+ docked vesicles at $t = 0$, i.e., just after the previous AP (see Fig 2). In terms of this conditional probability, the distribution $P_-^{ss}(n_-)$ in Eq. (1) is given by averaging $p(n, t_s|n'_+)$ over both the inter-spike interval t_s as well as the initial number n'_+. Note that we are using primed variables to distinguish variables at the *previous* AP from those at the current AP.

$$P_-^{ss}(n_-) = \sum_{n'_+} \int_0^\infty p\left(n_-, t_s|n'_+\right) P_+^{ss}(n'_+) g(t_s) dt_s, \tag{2}$$

where $P_+^{ss}(n'_+)$ is the steady-state probability distribution of having $n = n'_+$ just after an action potential. Since the distribution of ISIs is given experimentally, we need to calculate the other two distributions inside the integral on the right.

The conditional distribution $p(n, t|n'_+)$ of n between two successive action potentials describes the time-dependent replenishment process, and thus satisfies the corresponding Master equation [45],

$$\frac{\partial p(n, t|n'_+)}{\partial t} = k\left(M - (n-1)\right) p(n-1, t|n'_+) - k(M-n) p(n, t|n'_+). \tag{3}$$

This equation can be solved using the generating function $F(q, t|n'_+) = \sum_n q^n p(n, t|n'_+)$

(see SI Section 1 for the details), and we obtain the solution as,

$$p(n,t|n'_+) = \binom{M-n'_+}{n-n'_+}\left(1-e^{-kt}\right)^{n-n'_+} e^{-[k(M-n)]t}. \tag{4}$$

We next need to calculate $P_+^{ss}(n_+)$, the steady-state probability distribution of having n_+ docked vesicles *immediately after* the vesicle release. This is non-trivial since $n_+ = n_- - b$, and since n_- depends upon the n'_+ of the previous interval, the result for any interval depends upon the results of the previous interval. Starting with exact recursive relations between conditional probabilities P_+ after two successive APs (see Eq. (7) in section 2 of SI for details) in similar lines as [33,34], under the assumed conditions in steady state, we obtain a self-consistent equation for $P_+^{ss}(n_+)$.

$$P_+^{ss}(n_+) = \sum_{n'_+,b}\int_0^\infty dt_s g(t_s) p(n_+ + b, t_s|n'_+) B(n_+ + b, p_r, b) P_+^{ss}(n'_+). \tag{5}$$

Eq. (5) contains the unknown $P_+^{ss}(n_+)$ on both sides. Other quantities are known, including $p(n_+ + b, t_s|n'_+)$ (from Eq. (4)). In a difficult and lengthy calculation (see details in SI Section 3), we show that the corresponding generation function to the above distribution, namely $F_+(q) = \sum_{n_+=0}^{\infty} q^{n_+} P_+^{ss}(n_+)$ can be obtained using the knowledge of $F(q,t|n'_+)$, the generating function for $p(n,t|n'_+)$ mentioned above. This generating function leads us to the other two relevant generating functions $F_-(q) = \sum_{n_-=0}^{\infty} q^{n_-} P_-^{ss}(n_-)$ and $F_b(q) = \sum_{b=0}^{\infty} q^b Q^{ss}(b)$ corresponding to the distributions $P_-^{ss}(n_-)$ and $Q^{ss}(b)$. Since the three stochastic variables, n_-, n_+, and b are related to each other (namely $n_+ = n_- - b$), the generating functions must be too, and we can show that (see details in SI Section 4) they are related as:

$$F_-(q) = F_+\left(\frac{q-p_r}{1-p_r}\right) \text{ and } F_b(q) = F_+\left(\frac{p_r(q-1)}{1-p_r}+1\right). \tag{6}$$

From the knowledge of $F_b(q)$, we may finally obtain the desired distribution of quantal content $Q^{ss}(b)$ (see SI Section 4) using the standard relationship $Q^{ss}(b) =$

$\frac{1}{b!}\frac{\partial^b F_b(q)}{\partial q^b}\Big|_{q=0}$ [45]:

$$Q^{ss}(b) = \sum_{n=0}^{\infty}\binom{n}{b}(-1)^{n-b}\binom{M}{n}\frac{p_r^n}{1-(1-p_r)^n L_n}\Bigg[\phi_{n,0} + \sum_{\{S_{(n-1)}\}}\frac{(1-p_r)^{\sum_i m_i}\phi_{n,m_z}\phi_{m_z,m_{z-1}}\cdots\phi_{m_1,0}}{\prod_i(1-(1-p_r)^{m_i}L_{m_i})}\Bigg], \tag{7}$$

where,

$$\phi_{n,m} = \binom{n}{m}\int_0^\infty dt_s g(t_s)e^{-nkt_s}(e^{kt_s}-1)^{n-m}, \text{ and } L_n = \int_0^\infty dt_s g(t_s)e^{-nkt_s}.$$

Here $\{S_{(n-1)}\}$ denotes the set of all the subsets $S_{(n-1)} = \{m_i\} = (m_z, m_{z-1}, \cdots, m_1)$ with $m_i \in (1, 2, \cdots, n-1)$ such that $m_z > m_{z-1} > \cdots > m_1$. Although the upper limit of the sum is shown up to ∞, due to the combinatorial factor $\binom{M}{n}$, n never exceeds M. The closed form expressions of the mean and $CV^2 = \frac{\langle b^2\rangle}{\langle b\rangle^2} - 1$ of the distribution in Eq. (7) (see Section 4 in SI) are given by,

$$\langle b\rangle = \frac{Mp_r\phi_{1,0}}{1-(1-p_r)L_1}\text{ , and}$$

$$CV^2 = \frac{\phi_{1,0}+p_rL_1}{M\phi_{1,0}}\left[\frac{(M-1)}{1-(1-p_r)^2L_2}\left[\phi_{2,0}\left(1+\frac{p_rL_1}{\phi_{1,0}}\right)+(1-p_r)\phi_{2,1}\right]+\frac{1}{p_r}\right]-1 \tag{8}$$

Note that for an arbitrary $g(t_s)$ there is no reason to expect that $Q^{ss}(b)$ in Eq. (7) would reduce to a binomial distribution. As the number of subsets $S_{(n-1)}$ grows sharply with $n \in [b, M]$, the enumeration time of Eq. (7) may be large for large values of M. Using the software Mathematica, for $M \sim 15$, we could compute the distribution $Q^{ss}(b)$ for many different choices of $g(t_s)$ in approximately 30 minutes on a personal computer. Further analytical simplification of the formula is achievable for specific cases. We demonstrate this procedure by simplifying $Q^{ss}(b)$ for two special cases namely fixed ISIs (i.e. constant frequency stimulation), as well as exponentially distributed ISIs.

Fixed frequency AP train

When t_s *is deterministic*, we have an AP train at a fixed frequency $f = 1/T$, and $g(t_s) = \delta(t_s - T)$. When we substitute this in Eq. (7), we find (see details in SI Section 5(a)) that the expression for $Q^{ss}(b)$ reduces to a binomial distribution:

$$Q^{ss}(b) = B(M, p_{rb}, b) \tag{9}$$

$$\text{where, } p_{rb} = \frac{(1 - e^{-kT})p_r}{1 - (1 - p_r)e^{-kT}} \tag{10}$$

Thus the steady state quantal content distribution corresponding to a deterministic train of APs is indeed a binomial. However, Eq. (9) *is not equivalent to the approximate binomial often assumed in the literature, namely* $B(\langle n_- \rangle, p_r, b)$. In contrast the exact distribution has the parameters M and a modified release probability p_{rb} given by Eq. (10), which depends in the interval T and growth rate k apart from p_r. In fact we may calculate exactly $\langle n_- \rangle = Mp_{rb}/p_r$ now (see SI Section 5(a)), and use that to compute the approximate binomial formula $B(\langle n_- \rangle, p_r, b)$. We note that the result of the heuristic model presented in Ref. [20] is equivalent to Eq. (9) for this special case of constant frequency APs. In the low frequency limit (i.e. large T), from Eq. (10), $p_{rb} \to p_r$ (the release probability in the steady state), as one would expect.

Since Kinetic Monte Carlo simulations of the full stochastic growth and vesicle release process is expected to give a numerically accurate answer for the steady state distribution of the quantal content, we proceed to compare it with the exact distribution. In Fig 3, we see that the exact binomial distribution of $Q^{ss}(b)$ (Eq. (9)) matches perfectly the data from Kinetic Monte Carlo (KMC) simulations (code in SI) of this process (see the red symbols), while the approximate binomial $B(\langle n_- \rangle, p_r, b)$ deviates significantly. This validates the predicted difference between the exact and approximate binomial expressions.

The mean and CV^2 of the exact binomial distribution Eq. (9) are,

$$\langle b \rangle = Mp_{rb} \;\text{ and, }\; CV^2 = \frac{(1 - p_{rb})}{Mp_{rb}}, \tag{11}$$

We note that although the mean of the approximate binomial is $\langle n_- \rangle p_r = M p_{rb}$ (same as the exact binomial), its $CV^2 = \frac{(1-p_r)}{M p_{rb}}$ is clearly different from the exact CV^2 appearing in Eq. (11).

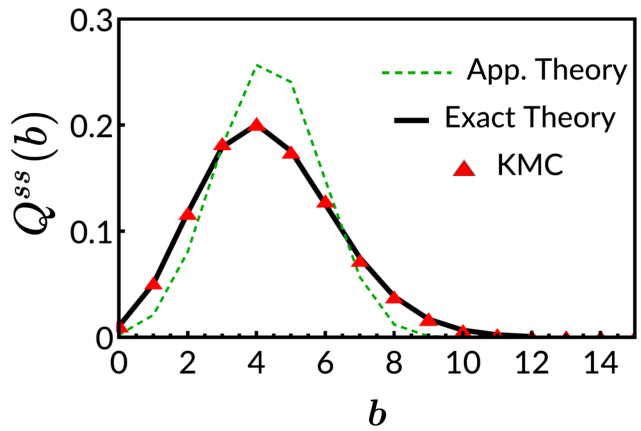

Fig 3: Burst size distribution under fixed AP arrival times. The exact (thick line) and approximate (dashed line) Binomial distributions (see text) of $Q^{ss}(b)$ for the case of deterministic intervals T of AP are plotted. The data from KMC simulations are shown in red symbols. The values of the parameters used are $M = 50$, $p_r = 0.5$, $k = 2$ sec^{-1} and $f = 1/T = 20$ Hz.

Exponentially distributed ISIs

When the *AP train is a Poisson process*, the interspike intervals are exponentially distributed, $g(t_s) = f_0 e^{-f_0 t_s}$. We can substitute this expression in Eqs. (7) and (8) to obtain (details in SI Section 5(b)) the following expression for the steady state quantal content distribution:

$$Q^{ss}(b) = \sum_{n=0}^{\infty} (-1)^{n-b} \binom{n}{b} \binom{M}{n} \frac{n!(kp_r)^n}{\prod_{i=1}^{n} (f_0 + ki - (1-p_r)^i f_0)}. \tag{12}$$

We can again calculate closed form expressions for the mean and CV^2 of the distribution in Eq. (12) (see Section 5(b) in SI):

$$\langle b \rangle = \frac{M k p_r}{k + f_0 p_r} \quad \text{and} \quad CV^2 = \frac{1}{M} \left(\frac{2(M-1)(k + f_0 p_r)}{2k + f_0 p_r (2 - p_r)} + \frac{f_0}{k} - M + \frac{1}{p_r} \right). \tag{13}$$

Note that this distribution is no longer a binomial. Thus even in one of the simplest cases of a stochastic $g(t_s)$, a systematic treatment of the stochasticity in n_- leads to a quantal content distribution that is non-binomial. It is instructive to ask whether the binomial distribution for fixed time intervals derived in Eq. (9) above may be used as an approximation for the Poisson case — one may think that roughly the inverse rate $1/f_0$ may be equated to a constant interval T. The fact that this does not work is shown in Fig 4 — while the numerically accurate Kinetic Monte Carlo data matches perfectly with the exact $Q^{ss}(b)$ from Eq. (12), the binomial formula (Eq. (9)) with $T = 1/f_0$ differs significantly.

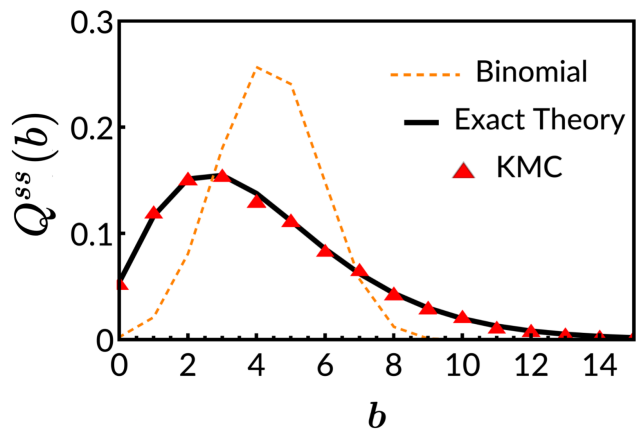

Fig 4: Burst size distribution under exponentially distributed AP arrival times. The exact distribution $Q^{ss}(b)$ for exponentially distributed AP intervals from Eq. (12) is shown as a solid line, and the Kinetic Monte Carlo simulation data are shown in red symbols. The Binomial distribution of Eq. (9) with $T \to 1/f_0$, shown by a dashed line, is far from the correct curves. The parameter values are $M = 50$, $p_r = 0.5$, $k = 2$ sec^{-1} and $f_0 = 20$ Hz.

Distribution of experimentally obtained quantal contents and comparison with theory

To validate the predictions of our model, we performed electrophysiological experiments (see the Materials and methods). The comparison between theory and experiment is done in Fig 5. In Figs 5a and 5b, for synapse-1 (left) and synapse-2

(right) respectively, we plot the time-varying fluctuating quantal contents for a single tetanic burst (in blue), as well as the mean quantal content over 20 repeats (in red). In both neurons the mean quantal content reaches a steady-state value beyond 0.8 s (see the yellow box). Considering quantal contents between times $0.8 - 1.0$ s over all the 20 histories, we obtained the normalised histogram of the experimental quantal contents – these are shown (in green) in Figs 5c and 5d.

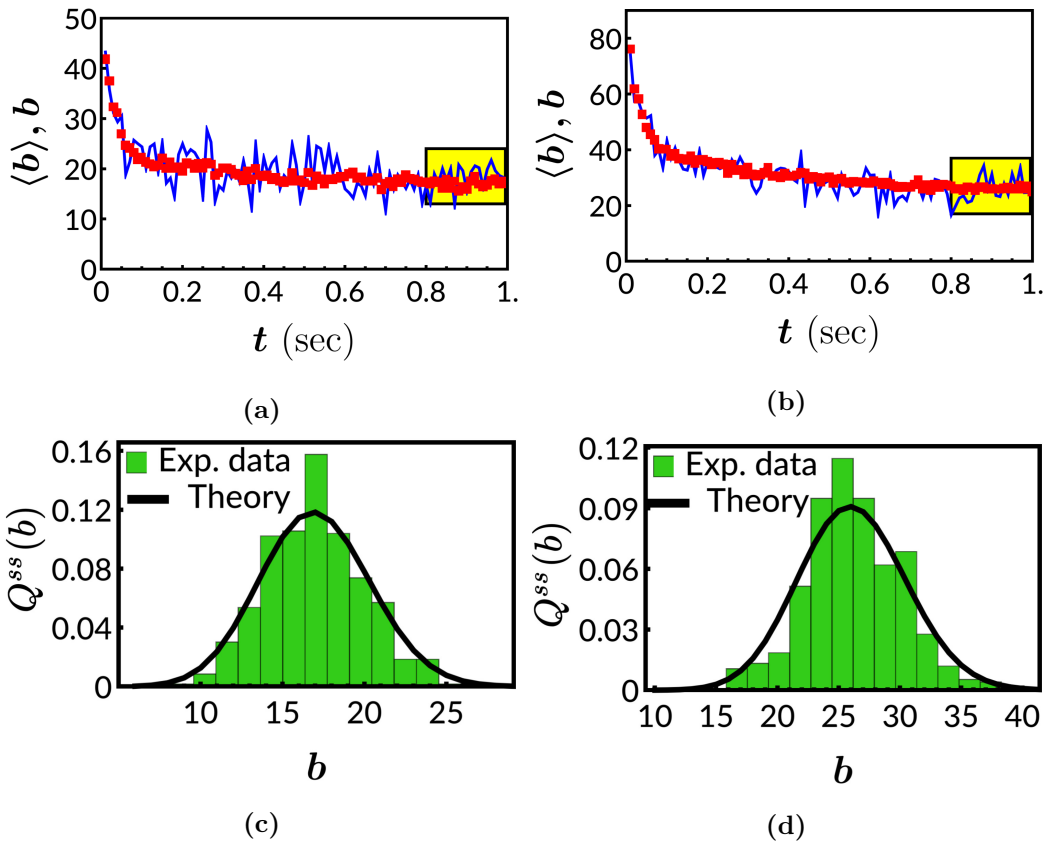

Fig 5: Comparing experimental distributions with predictions. The experimental mean quantal content $\langle b \rangle$ is plotted (in red) against time, for (a) synapse-1 and (b) synapse-2. The blue curves represent one of the 20 experimental realizations of the quantal content. The yellow box shows the part of data we considered to be in the steady state for plotting the experimental histograms of quantal content in (c) and (d) (in green). In (c) and (d), the parameter values used for the exact theoretical distributions (black curves) for synapse-1 are $M = 50$ and $p_{rb} = 0.345$ and for the synapse-2 are $M = 98$ and $p_{rb} = 0.266$.

To compare the experimental data with the exact distribution Eq. (9), we first

needed to estimate the parameters M and p_{rb} from experiments. We know that after the first AP (at 0 sec), the quantal content b_0 follows a binomial distribution $B(M, p_{r0}, b_0)$, with a mean Mp_{r0} and variance $Mp_{r0}(1 - p_{r0})$. From the 20 experimental histories we obtained the mean and variance of b_0 and using the theoretical formulas, obtained M by eliminating p_{r0}. Next we equate the experimental mean quantal content (corresponding to the data in Figs 5c and 5d) in the steady state, to the theoretical mean $\langle b \rangle = Mp_{rb}$ (Eq. (11)), and determine p_{rb}. With these parameters, we plot the exact distribution Eq. (9) and they match quite well to the experimental data in Figs 5c and 5d (black curves). Note that we did not have to separately match the variance of the data and theory to obtain the fitted distribution. The experimental and theoretical CV^2 automatically turn out quite close. For synapse-1, the theory predicts 0.039 vs the experimental value of 0.032, while for synapse-2, the values are 0.028 (theory) vs 0.022 (experiment). The steady state values of p_r, k and T were not separately necessary to make the theory-experiment comparison, as they combine to give a single parameter p_{rb} which is sufficient.

Poisson-like statistics have been observed in the ISI distribution from neurons in the visual cortex [40,41]. Since we have a prediction for the quantal content distribution under these circumstances, it would be interesting to test it experimentally by using Poissonian AP stimulations, and estimate the parameters (p_r, k) using that data. For that purpose, the explicit formulae for the theoretical moments from Eq. (13) may be used.

Frequency dependence of mean quantal content in the steady state – comparing theory to experiments

For a spike train at fixed time intervals T, the parameter p_{rb} (Eq. (10)) associated with the binomial and hence the mean quantal content $\langle b \rangle = Mp_{rb}$ (Eq. (11)) follow a certain dependence on the frequency of stimulation $f = 1/T$. Experimental data for $\langle b \rangle$ as a function of f is available as published results in Ref. [38] for three different synapse types – two hippocampal (CA3 - CA1 and EC - DG) and one

auditory (MNTB - LSO). The evoked postsynaptic currents were converted to $\langle b \rangle$ using appropriate quantal sizes. For each of the three synapse types, the values of p_r and the maximum vesicle docking rates kM are experimentally known [38]. Since we do not know the values of M and k separately, we do a one parameter fit with varying k to get the least square difference between the theoretical and experimental curves of $\langle b \rangle$ versus f. The best fit values of the parameter k and M thus obtained for the three synapse types are provided in the caption of Fig 6, and plots of the theoretical $\langle b \rangle$ (solid lines) are shown against the experimental values as a function of f. The extent of match demonstrates the usefulness of the exact formula (Eqs. (10,11)) for the frequency dependence of the mean quantal content in the steady state.

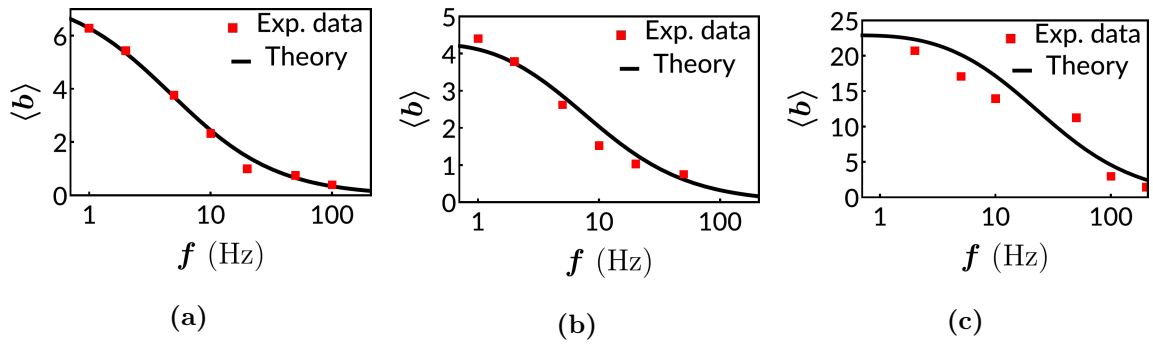

Fig 6: Comparing experimental frequency dependence of the mean quantal content with model fits. The frequency dependence of the theoretical mean quantal content is matched with the experimental values, for the synapse types (a) CA3-CA1, (b) EC-DG, and (c) MNTB-LSO. The experimental data was extracted from Ref. [38]. The theoretical curves were calculated using the parameter values obtained from the data provided in [38], followed by a one-parameter fit. The parameters are as follows: (a) $M = 688$, $p_r = 0.011$, $k = 0.0523$ sec^{-1} (b) $M = 17$, $p_r = 0.251$, $k = 2.058$ sec^{-1} (c) $M = 147$, $p_r = 0.156$, $k = 3.816$ sec^{-1}

Discussion

We make three basic biological assumptions in our work here, in line with much of the theoretical literature. (i) Our results apply when the quantal content distribution has reached a steady state, and we do not consider the dynamics during the period of short-term plasticity before a steady state is achieved, shown by the region where $\langle b \rangle$ decays in Figs 5a and 5b. (ii) We assume that the rate of replenishment is proportional to the number of empty docking sites. We do not therefore consider complexities in the replenishment process, for eg. pre-synaptic homeostasis [42, 46–49]. Many of these processes are compatible with the assumption of an approximately constant rate of replenishment, k, and our model is appropriate under this condition. (iii) Along with much of the literature, our model also assumes that the release probabilities of the vesicles, p_r is a constant during steady-state signaling at the pre-synaptic terminal. Recent advancements in the ultrastructural analysis of the neurons have suggested however that the release probabilities may be spatially heterogeneous [50, 51], which we do not consider in this work.

Incorporation of these additional complexities into a stochastic model of vesicle release is certainly possible in theory, but is likely to be a harder problem than the model solved here. However, as our paper shows, a careful accounting of coupled stochastic processes is necessary to obtain theoretically robust results. For steady-state processes in particular, this involves properly summing over stochastic trajectories. Since the quantal theory of neurotransmitter release, first proposed by Castillo et al. [4], it has been known that the vesicle release process is stochastic, and at least since 1975, it has often been assumed that the statistics of vesicle release can be described by binomial distributions. For a model of quantal release with a probability of release p_r and n_- vesicles standing ready to be released, the statistics of vesicle release will be described by $B(n_-, p_r, b)$. However, n_- itself is a stochastic variable that depends upon the processes of replenishing the RRP, as well as the time distribution of arrival times, $g(t_s)$, of the action potential at the pre-synaptic terminal. The steady-state distribution of the quantal content therefore depends

upon these coupled stochastic processes.

In this paper, we successfully perform this calculation, which yields a formula, Eq. (7), for the probability distribution of the quantal contents under the assumption of a reasonable kinetic replenishment model and arbitrary $g(t_s)$. We also derive exact expressions for the mean and CV^2 of this general distribution (Eq. (8)). Using this formula, we show that when the arrival time of the APs are not fixed but follow the simplest random process, a Poisson process, the resultant quantal content distribution deviates significantly from the binomial distribution. Eqs. (12) and (13) are important predictions for exponentially distributed ISIs, that would be very interesting to compare to experiments, and estimate model parameters.

Under the specific assumption of fixed arrival times of the APs, we find that Eq. (7) reduces to the binomial distribution given by Eq. (9). While this is in qualitative agreement with experiments performed under these conditions, it has typically been assumed previously that the binomial probability parameter of these empirical distributions is the same as the intrinsic probability of release from the post-synaptic terminal, p_r, and the size parameter is equivalent to the average size of the RRP, $\langle n_- \rangle$. Here we show by exact calculation that the relevant binomial parameter of the distribution is not p_r but a different parameter p_{rb}, given by Eq. (10), and the size parameter is M, not the average but the maximum size of the RRP.

More generally, Eq. (7) is a prediction for the statistics of quantal release when the inter-spike timing of AP trains obey any probability distribution $g(t_s)$. This is significant for neuronal transmission *in vivo* because neural information is believed to be transmitted through differences in spiking rates [3]. Our results should thus be extremely useful for studying synaptic transmission under more physiologically realistic conditions.

Materials and Methods

Details of the derivations for analytical results are described in Appendices 1, 2, 3, 4, 5, 6, and 7.

We performed electrophysiological experiments in acute brainstem slices of juvenile mice (postnatal day 11) at MNTB-LSO synapses. These fast auditory synapses transfer inhibitory glycinergic information and can maintain reliable neurotransmission even during prolonged high-frequency stimulation [52,53]. We refer the reader to the Methods section of Ref. [53] for details on the slice preparation and details of whole-cell patch-clamp recordings. The stimulation protocol consisted of repetitive tetanic AP bursts (100 Hz, 1 s) that were given 20 times. A 30-s rest period was introduced between repeats to allow for recovery from short-term depression. The number of fused SVs was determined as the ratio of the peak amplitude of evoked inhibitory postsynaptic currents (eIPSC) to the current produced by a single quantum (q) [pA/(pA/SV)]. Detailed information is available in Refs. [53,54].

Supporting information

SI File (PDF)—: (1) Sections 1-4: Shows the mathematical steps involved in the derivation of the distribution of quantal content and its moments. (2) Sections 5-7: The extension to the special cases of constant ISI and Poisson AP trains, with proofs of the necessary mathematical identities used. (3) Section 8: Explains the idea of approach to steady state of model parameters as a function of time. (4) Section 9: KMC code used for Figs. (3) and (4) in the main manuscript.

Acknowledgements

DD acknowledges IIT Bombay for funding. KR thanks IIT Bombay for Institute Ph.D. fellowship. AS acknowledges support by NIH/NIDCD grant R01DC019268. EF acknowledges support by Bundesministerium für Bildung und Forschung grant 01GQ2001.

Author Contributions

Conceptualization: Krishna Rijal, Abhyudai Singh, Ashok Prasad, and Dibyendu Das

Formal analysis: Krishna Rijal, Abhyudai Singh, Ashok Prasad, and Dibyendu Das

Funding acquisition: Abhyudai Singh, Eckhard Friauf, and Dibyendu Das

Investigation: Krishna Rijal, Nicolas I.C. Müller, Eckhard Friauf, Abhyudai Singh, Ashok Prasad, and Dibyendu Das

Methodology: Krishna Rijal, Abhyudai Singh, Ashok Prasad, and Dibyendu Das

Software: Krishna Rijal

Supervision: Ashok Prasad, Eckhard Friauf, and Dibyendu Das

Writing – original draft: Krishna Rijal, Ashok Prasad, and Dibyendu Das

Writing – review & editing: Krishna Rijal, Nicolas I.C. Müller, Eckhard Friauf, Abhyudai Singh, Ashok Prasad, and Dibyendu Das

Competing interests

The authors declare no competing interests.

References

[1] S. Herculano-Houzel, "The human brain in numbers: a linearly scaled-up primate brain," *Front Hum Neurosci*, vol. 3, p. 31, 2009.

[2] Y. Tang, J. R. Nyengaard, D. M. De Groot, and H. J. Gundersen, "Total regional and global number of synapses in the human brain neocortex," *Synapse*, vol. 41, no. 3, pp. 258–73, 2001.

[3] E. R. Kandel, J. Koester, S. Mack, and S. Siegelbaum, *Principles of neural science*. New York: McGraw Hill, sixth edition. ed., 2021.

[4] J. Del Castillo and B. Katz, "Quantal components of the end-plate potential," *The Journal of Physiology*, vol. 124, no. 3, p. 560, 1954.

[5] V. N. Murthy and P. De Camilli, "Cell biology of the presynaptic terminal," *Annu Rev Neurosci*, vol. 26, pp. 701–28, 2003.

[6] S. O. Rizzoli and W. J. Betz, "Synaptic vesicle pools," *Nat Rev Neurosci*, vol. 6, no. 1, pp. 57–69, 2005.

[7] A. A. Alabi and R. W. Tsien, "Synaptic vesicle pools and dynamics," *Cold Spring Harb Perspect Biol*, vol. 4, no. 8, p. a013680, 2012.

[8] E. Neher, "Merits and limitations of vesicle pool models in view of heterogeneous populations of synaptic vesicles," *Neuron*, vol. 87, no. 6, pp. 1131–1142, 2015.

[9] S. Weis, R. Schneggenburger, and E. Neher, "Properties of a model of ca++-dependent vesicle pool dynamics and short term synaptic depression," *Biophysical Journal*, vol. 77, no. 5, pp. 2418–2429, 1999.

[10] D. A. Rusakov, L. P. Savtchenko, and P. E. Latham, "Noisy synaptic conductance: Bug or a feature?," *Trends in Neurosciences*, vol. 43, no. 6, pp. 363–372, 2020.

[11] M. S. Goldman, "Enhancement of information transmission efficiency by synaptic failures," *Neural Computation*, vol. 16, no. 6, pp. 1137–1162, 2004.

[12] C. Zhang and C. S. Peskin, "Improved signaling as a result of randomness in synaptic vesicle release," *Proceedings of the National Academy of Sciences*, vol. 112, no. 48, pp. 14954–14959, 2015.

[13] M. V. Tsodyks and H. Markram, "The neural code between neocortical pyramidal neurons depends on neurotransmitter release probability," *Proceedings of the National Academy of Sciences*, vol. 94, no. 2, pp. 719–723, 1997.

[14] J. S. Dittman and W. G. Regehr, "Calcium dependence and recovery kinetics of presynaptic depression at the climbing fiber to purkinje cell synapse," *Journal of Neuroscience*, vol. 18, no. 16, pp. 6147–6162, 1998.

[15] J. S. Dittman, A. C. Kreitzer, and W. G. Regehr, "Interplay between facilitation, depression, and residual calcium at three presynaptic terminals," *Journal of Neuroscience*, vol. 20, no. 4, pp. 1374–1385, 2000.

[16] E. M. McLachlan, "The statistics of transmitter release at chemical synapses," *Int Rev Physiol*, vol. 17, pp. 49–117, 1978.

[17] S. Redman, "Quantal analysis of synaptic potentials in neurons of the central nervous system.," *Physiological Reviews*, vol. 70, no. 1, pp. 165–198, 1990.

[18] A. Arleo, T. Nieus, M. Bezzi, A. d'Errico, E. d'Angelo, and O. J.-M. Coenen, "How synaptic release probability shapes neuronal transmission: information-theoretic analysis in a cerebellar granule cell," *Neural Computation*, vol. 22, no. 8, pp. 2031–2058, 2010.

[19] R. Rosenbaum, J. Rubin, and B. Doiron, "Short term synaptic depression imposes a frequency dependent filter on synaptic information transfer," *PLoS Computational Biology*, vol. 8, no. 6, p. e1002557, 2012.

[20] C. Pulido, F. F. Trigo, I. Llano, and A. Marty, "Vesicular release statistics and unitary postsynaptic current at single gabaergic synapses," *Neuron*, vol. 85, no. 1, pp. 159–172, 2015.

[21] G. Malagon, T. Miki, I. Llano, E. Neher, and A. Marty, "Counting vesicular release events reveals binomial release statistics at single glutamatergic synapses," *Journal of Neuroscience*, vol. 36, no. 14, pp. 4010–4025, 2016.

[22] Z. Vahdat, Z. Xu, and A. Singh, "Modeling and characterization of neuronal synapses using stochastic hybrid systems," in *2019 IEEE 58th Conference on Decision and Control (CDC)*, pp. 4729–4734, IEEE, 2019.

[23] M. D. Miyamoto, "Binomial analysis of quantal transmitter release at glycerol treated frog neuromuscular junctions," *J Physiol*, vol. 250, pp. 121–42, Aug 1975.

[24] R. Malinow and R. W. Tsien, "Presynaptic enhancement shown by whole-cell recordings of long-term potentiation in hippocampal slices," *Nature*, vol. 346, pp. 177–80, Jul 1990.

[25] S. S. Kelly and N. Robbins, "Statistics of neuromuscular transmitter release in young and old mouse muscle," *The Journal of Physiology*, vol. 385, pp. 507–16, Apr 1987.

[26] R. A. Silver, A. Momiyama, and S. G. Cull-Candy, "Locus of frequency-dependent depression identified with multiple-probability fluctuation analysis at rat climbing fibre-purkinje cell synapses," *The Journal of Physiology*, vol. 510, no. 3, pp. 881–902, 1998.

[27] H. Taschenberger, V. Scheuss, and E. Neher, "Release kinetics, quantal parameters and their modulation during short-term depression at a developing synapse in the rat cns," *The Journal of Physiology*, vol. 568, no. 2, pp. 513–537, 2005.

[28] E. Hanse and B. Gustafsson, "Paired-pulse plasticity at the single release site level: an experimental and computational study," *Journal of Neuroscience*, vol. 21, no. 21, pp. 8362–8369, 2001.

[29] C. Pulido and A. Marty, "Quantal fluctuations in central mammalian synapses: functional role of vesicular docking sites," *Physiological Reviews*, vol. 97, no. 4, pp. 1403–1430, 2017.

[30] G. Malagon, T. Miki, V. Tran, L. C. Gomez, and A. Marty, "Incomplete vesicular docking limits synaptic strength under high release probability conditions," *eLife*, vol. 9, p. e52137, 2020.

[31] A. Brémaud, D. C. West, and A. M. Thomson, "Binomial parameters differ across neocortical layers and with different classes of connections in adult rat

and cat neocortex," *Proceedings of the National Academy of Sciences*, vol. 104, no. 35, pp. 14134–14139, 2007.

[32] H. Wen, M. J. McGinley, G. Mandel, and P. Brehm, "Nonequivalent release sites govern synaptic depression," *Proceedings of the National Academy of Sciences*, vol. 113, no. 3, pp. E378–E386, 2016.

[33] A. Barri, Y. Wang, D. Hansel, and G. Mongillo, "Quantifying repetitive transmission at chemical synapses: a generative-model approach," *ENeuro*, vol. 3, no. 2, 2016.

[34] A. D. Bird, M. J. Wall, and M. J. Richardson, "Bayesian inference of synaptic quantal parameters from correlated vesicle release," *Frontiers in Computational Neuroscience*, vol. 10, p. 116, 2016.

[35] O. Bykowska, C. Gontier, A.-L. Sax, D. W. Jia, M. L. Montero, A. D. Bird, C. Houghton, J.-P. Pfister, and R. P. Costa, "Model-based inference of synaptic transmission," *Frontiers in Synaptic Neuroscience*, vol. 11, p. 21, 2019.

[36] C. Gontier, S. C. Surace, and J.-P. Pfister, "Bayesian active learning for closed-loop synaptic characterization," *arXiv preprint arXiv:2201.07539*, 2022.

[37] K. Mahfooz, M. Singh, R. Renden, and J. F. Wesseling, "A well-defined readily releasable pool with fixed capacity for storing vesicles at calyx of held," *PLoS Computational Biology*, vol. 12, no. 4, p. e1004855, 2016.

[38] E. G. Krächan, A. U. Fischer, J. Franke, and E. Friauf, "Synaptic reliability and temporal precision are achieved via high quantal content and effective replenishment: auditory brainstem versus hippocampus," *The Journal of Physiology*, vol. 595, no. 3, pp. 839–864, 2017.

[39] R. P. Costa, P. J. Sjöström, and M. C. Van Rossum, "Probabilistic inference of short-term synaptic plasticity in neocortical microcircuits," *Frontiers in Computational Neuroscience*, vol. 7, p. 75, 2013.

[40] M. N. Shadlen and W. T. Newsome, "The variable discharge of cortical neurons: implications for connectivity, computation, and information coding," *Journal of Neuroscience*, vol. 18, no. 10, pp. 3870–3896, 1998.

[41] G. Maimon and J. A. Assad, "Beyond poisson: Increased spike-time regularity across primate parietal cortex," *Neuron*, vol. 62, no. 3, pp. 426–440, 2009.

[42] J. S. Lee, W.-K. Ho, E. Neher, and S.-H. Lee, "Superpriming of synaptic vesicles after their recruitment to the readily releasable pool," *Proceedings of the National Academy of Sciences*, vol. 110, no. 37, pp. 15079–15084, 2013.

[43] K. Ikeda and J. M. Bekkers, "Counting the number of releasable synaptic vesicles in a presynaptic terminal," *Proceedings of the National Academy of Sciences USA*, vol. 106, no. 8, pp. 2945–50, 2009.

[44] B. G. Wilhelm, S. Mandad, S. Truckenbrodt, K. Kröhnert, C. Schäfer, B. Rammner, S. J. Koo, G. A. Claßen, M. Krauss, V. Haucke, H. Urlaub, and S. O. Rizzoli, "Composition of isolated synaptic boutons reveals the amounts of vesicle trafficking proteins," *Science*, vol. 344, no. 6187, pp. 1023–1028, 2014.

[45] C. W. Gardiner, *Handbook of stochastic methods*, vol. 3. springer Berlin, 1985.

[46] G. W. Davis, "Homeostatic control of neural activity: From phenomenology to molecular design," *Annual Review of Neuroscience*, vol. 29, no. 1, pp. 307–323, 2006. PMID: 16776588.

[47] H. Taschenberger, A. Woehler, and E. Neher, "Superpriming of synaptic vesicles as a common basis for intersynapse variability and modulation of synaptic strength," *Proceedings of the National Academy of Sciences*, vol. 113, no. 31, pp. E4548–E4557, 2016.

[48] J. M. Ortega, O. Genc, and G. W. Davis, "Molecular mechanisms that stabilize short term synaptic plasticity during presynaptic homeostatic plasticity," *eLife*, vol. 7, p. e40385, nov 2018.

[49] B. O. Orr, R. D. Fetter, and G. W. Davis, "Activation and expansion of presynaptic signaling foci drives presynaptic homeostatic plasticity," *Neuron*, 2022.

[50] D. Keller, N. Babai, O. Kochubey, Y. Han, H. Markram, F. Schürmann, and R. Schneggenburger, "An exclusion zone for ca2+ channels around docked vesicles explains release control by multiple channels at a cns synapse," *PLoS Computational Biology*, vol. 11, no. 5, p. e1004253, 2015.

[51] Y. Nakamura, H. Harada, N. Kamasawa, K. Matsui, J. S. Rothman, R. Shigemoto, R. A. Silver, D. A. DiGregorio, and T. Takahashi, "Nanoscale distribution of presynaptic ca2+ channels and its impact on vesicular release during development," *Neuron*, vol. 85, no. 1, pp. 145–158, 2015.

[52] S. E. Brill, A. Maraslioglu, C. Kurz, F. Kramer, M. F. Fuhr, A. Singh, and E. Friauf, "Glycinergic transmission in the presence and absence of functional glyt2: Lessons from the auditory brainstem," *Frontiers in Synaptic Neuroscience*, vol. 12, p. 560008, 2020.

[53] N. I. C. Müller, I. Paulussen, L. N. Hofmann, J. O. Fisch, A. Singh, and E. Friauf, "Development of synaptic fidelity and action potential robustness at an inhibitory sound localization circuit: effects of otoferlin-related deafness," *The Journal of Physioloy*, vol. 600, no. 10, pp. 2461–2497, 2022.

[54] N. I. C. Müller, M. Sonntag, A. Maraslioglu, J. J. Hirtz, and E. Friauf, "Topographic map refinement and synaptic strengthening of a sound localization circuit require spontaneous peripheral activity," *The Journal of Physiology*, vol. 597, no. 22, pp. 5469–5493, 2019.

Exact distribution of the quantal content in synaptic transmission Supplementary Information File

Krishna Rijal[a], Nicolas I.C. Müller[b], Eckhard Friauf[b], Abhyudai Singh[c], Ashok Prasad[d,1], and Dibyendu Das[a,1]

[a]Department of Physics, Indian Institute of Technology Bombay, Powai, Mumbai 400076, India
[b]Animal Physiology Group, Department of Biology, University of Kaiserslautern, Kaiserslautern, Germany
[c]Departments of Electrical and Computer Engineering, Biomedical Engineering and Mathematical Sciences, University of Delaware, Newark, DE 19716, USA
[d]Department of Chemical and Biological Engineering, Colorado State University, Fort Collins, Colorado, USA
[1]To whom correspondence should be addressed: dibyendu@phy.iitb.ac.in; ashok.prasad@colostate.edu

April 18, 2023

1 Probability distribution of docked vesicle number n between two consecutive action potentials

Let $p(n, t|n'_+)$ denote the probability distribution of the number n of docked (ready to release) vesicles at time t, starting from $n = n'_+$ at $t = 0$ (i.e. from the instant of the last action potential (AP)). Thus t denotes any time up to the next AP, i.e. $t < t_s$ where t_s is a time when the next AP arrives. In the interval t to $t+dt$, the number of docked vesicles may increase from $n-1$ to n with the probability $k(M-(n-1))dt$. Here k is the growth rate per empty docking sites, and M is maximum number of docking sites. Consequently, the master equation for the time evolution of $p(n, t|n'_+)$ between two successive APs is:

$$\frac{\partial p(n, t|n'_+)}{\partial t} = k\left(M-(n-1)\right)p(n-1, t|n'_+) - k(M-n)p(n, t|n'_+) \tag{1}$$

We define a generating function for the above probability distribution:

$$F(q, t|n'_+) = \sum_n q^n p(n, t|n'_+) \tag{2}$$

Here the limits of the above sum are $n'_+ \leq n \leq M$. Otherwise, we assume $p(n, t|n'_+) = 0$ if n'_+ falls outside this range. Multiplying Eq. (1) by $\sum_n q^n$ on both sides, we get a PDE for the generating function F:

$$\begin{aligned}\frac{\partial F}{\partial t} =& + kM\sum_n q^n p(n-1, t|n'_+) - k\sum_n q^n (n-1)p(n-1, t|n'_+) \\ &- kM\sum_n q^n p(n, t|n'_+) + k\sum_n q^n np(n, t|n'_+) = kMqF - kq^2\frac{\partial F}{\partial q} - kMF + kq\frac{\partial F}{\partial q}\end{aligned}$$

Rearranging the terms, we have,

$$\frac{\partial F}{\partial t} + kq(q-1)\frac{\partial F}{\partial q} = kM(q-1)F \tag{3}$$

We use the method of Lagrange characteristics to solve the Eq. (3). The result is:

$$F(q,t|n'_+) = q^M \left[1 - \frac{(q-1)}{q} e^{-kt}\right]^{M-n'_+} \tag{4}$$

We do binomial expansion of Eq. (4) to get

$$\begin{aligned} F =& q^{n'_+} \left[q(1-e^{-kt}) + e^{-kt}\right]^{M-n'_+} \\ =& \sum_{n=0}^{M-n'_+} \binom{M-n'_+}{n} \left[q^{n+n'_+} \left(1-e^{-kt}\right)^n\right] \left(e^{-kt}\right)^{M-n'_+-n} \end{aligned}$$

and relabelling $n + n'_+ \to n$ we get

$$F = \sum_{n=n'_+}^{M} \binom{M-n'_+}{n-n'_+} q^n \left(1-e^{-kt}\right)^{n-n'_+} \left(e^{-kt}\right)^{M-n} \tag{5}$$

Next we can compare Eq. (5) with Eq. (2) to get the expression of $p(n,t|n'_+)$:

$$\boxed{p(n,t|n'_+) = \binom{M-n'_+}{n-n'_+} \left(1-e^{-kt}\right)^{n-n'_+} e^{-[k(M-n)]t}} \tag{6}$$

for $n'_+ \leq n < \infty$. Note that for $n > M$, the probability goes to zero automatically in the above expression.

2 Self-consistent equation for the quantal content distribution $P_+^{ss}(n_+)$ in the steady state

Let us denote the time intervals between $(m-1)^{th}$ AP and m^{th} AP by t_{sm} and between the $(m-2)^{th}$ AP and $(m-1)^{th}$ AP by t_{sm-1}. We first relate the probability $P_+^m(n_{+,m}, t_{sm})$ of having $n_{+,m}$ number of docked vesicles after the mth AP, to the probability $P_+^{m-1}(n_{+,m-1}, t_{sm-1})$ of having $n_{+,m-1}$ number of vesicles just after the $(m-1)^{th}$ AP. To do so, we need to sum over all possible paths beginning at $n = n_{+,m-1}$ after the $(m-1)^{th}$ action potential and ending at $n = n_{+,m}$ after the mth AP.

The sum involves the product of three probabilities due to a sequence of steps: (i) initial $P_+^{m-1}(n_{+,m-1}, t_{sm-1})$, then (ii) the probability $p(n_{+,m} + b, t_{sm}|n_{+,m-1})$ that $n_{+,m-1}$ rises to $n_{+,m} + b$ in time t_{sm}, and (iii) finally the probability that at t_{sm}, the number $n_{+,m} + b$ of docked vesicles suddenly reduce to $n_{+,m}$ due to the AP triggered vesicle release, with the associated quantal content b being binomially distribution $B(n_{+,m}+b, p_r, b)$. After summing over all possible initial number $n_{+,m-1}$ and quantal content b we have,

$$P_+^m(n_{+,m}, t_{sm}) = \sum_{n_{+,m-1},b} B(n_{+,m}+b, p_r, b)p(n_{+,m}+b, t_{sm}|n_{+,m-1})P_+^{m-1}(n_{+,m-1}, t_{sm-1}) \tag{7}$$

We may follow the same procedure for $P_+^{m-1}(n_{+,m-1}, t_{sm-1})$ and so on, and build up a hierarchy of relations for any interval between two APs. The problem remains hard to solve as result for every interval depends on the history of the previous interval. We are particularly interested in the steady state attained after several APs appear, i.e. $m \gg 1$ and the output quantal contents statistically stabilise. We integrate Eq. (7) over the joint probability distribution $g_2(t_{sm}, t_{sm-1})$ of t_{sm} and t_{sm-1}. We get

$$\begin{aligned}
&\int_0^\infty \int_0^\infty dt_{sm} dt_{sm-1} g_2(t_{sm}, t_{sm-1}) P_+^m(n_{+,m}, t_{sm}) \\
=&\int_0^\infty \int_0^\infty dt_{sm} dt_{sm-1} g_2(t_{sm}, t_{sm-1}) \\
&\times \sum_{n_{+,m-1},b} p(n_{+,m} + b, t_{sm}|n_{+,m-1}) B(n_{+,m} + b, p_r, b) P_+^{m-1}(n_{+,m-1}, t_{sm-1})
\end{aligned} \tag{8}$$

If the interspike intervals (ISIs) are not correlated, we would have $g_2(t_{sm}, t_{sm-1}) = g(t_{sm})g(t_{sm-1})$, where $g(t_{sm})$ and $g(t_{sm-1})$ are the normalised distributions of t_{sm} and t_{sm-1} respectively. Then,

$$\begin{aligned}
&\int_0^\infty \int_0^\infty dt_{sm} dt_{sm-1} g(t_{sm}) g(t_{sm-1}) P_+^m(n_{+,m}, t_{sm}) \\
=&\int_0^\infty \int_0^\infty dt_{sm} dt_{sm-1} g(t_{sm}) g(t_{sm-1})
\end{aligned}$$

$$
\begin{aligned}
&\times \sum_{n_{+,m-1},b} p(n_{+,m}+b, t_{sm}|n_{+,m-1}) B(n_{+,m}+b, p_r, b) P_+^{m-1}(n_{+,m-1}, t_{sm-1}) \\
\Rightarrow &\int_0^\infty dt_{sm} g(t_{sm}) P_+^m(n_{+,m}, t_{sm}) \\
= &\sum_{n_{+,m-1},b} \int_0^\infty dt_{sm} g(t_{sm}) p(n_{+,m}+b, t_{sm}|n_{+,m-1}) B(n_{+,m}+b, p_r, b) \\
&\times \int_0^\infty dt_{sm-1} g(t_{sm-1}) P_+^{m-1}(n_{+,m-1}, t_{sm-1}) \qquad (9)
\end{aligned}
$$

In the long time limit, the steady state probability distribution of vesicle number after any AP is $P_+^{ss}(n_{+,m}) = \int_0^\infty dt_{sm-1} g(t_{sm-1}) P_+^{m-1}(n_{+,m-1}, t_{sm-1})$, which does not depend any more on the exact history of the spike train. Dropping the subscripts m (in the steady state), and setting $t_{sm} = t_s$ and $n_{+,m-1} = n'_+$, the Eq. (9) becomes

$$
\boxed{P_+^{ss}(n_+) = \sum_{n'_+,b} \int_0^\infty dt_s g(t_s) p(n_+ + b, t_s|n'_+) B(n_+ + b, p_r, b) P_+^{ss}(n'_+)} \qquad (10)
$$

Note that this is a self-consistent equation for the unknown $P_+^{ss}(n_+)$, when we know $g(t_s)$, $B(n_+ + b, p_r, b)$ and $p(n_+ + b, t_s|n'_+)$ (Eq. (6)). This equation appears in the main manuscript. We analytically treat it in the next section.

3 Generating function of the distribution $P_+^{ss}(n_+)$ in the steady state

We define a generating function of $P_+^{ss}(n_+)$ as follows and solve it in this section:

$$
F_+(q) = \sum_{n_+} q^{n_+} P_+^{ss}(n_+) \qquad (11)
$$

In Eq. (10), the limits of the summation are $0 \le b \le M - n_+$ and $0 \le n'_+ \le n_+ + b$. Since anyways, $p(n_+ + b, t_s|n'_+) = 0$ outside the limits (see Eq. (6)), we may as well use the range $0 \le b, n'_+ \le \infty$. Multiplying Eq. (10) by q^{n_+} and summing over n_+

(with $0 \leq n_+ \leq \infty$), we have:

$$F_+(q) = \sum_{n'_+,b} \int_0^\infty dt_s g(t_s) \sum_{n_+} q^{n_+} p(n_+ + b, t_s|n'_+) B(n_+ + b, p_r, b) P_+^{ss}(n'_+) \tag{12}$$

We introduce a new variable $\tilde{n_+} = n_+ + b$ with $b \leq \tilde{n_+} \leq \infty$. Note that $B(\tilde{n_+}, p_r, b) = 0$ for $\tilde{n_+} < b$, so we may keep the range $0 \leq \tilde{n_+} \leq \infty$.

$$F_+(q) = \int_0^\infty dt_s g(t_s) \sum_{n'_+,b} \sum_{\tilde{n_+}} q^{\tilde{n_+}-b} p(\tilde{n_+}, t_s|n'_+) B(\tilde{n_+}, p_r, b) P_+^{ss}(n'_+) \tag{13}$$

Summing over b after substituting $B(\tilde{n_+}, p_r, b) = \binom{\tilde{n_+}}{b} p_r^b (1-p_r)^{\tilde{n_+}-b}$, we have

$$\begin{aligned} F_+(q) &= \int_0^\infty dt_s g(t_s) \sum_{n'_+} \sum_{\tilde{n_+}} \left(1 - p_r + \frac{p_r}{q}\right)^{\tilde{n_+}} q^{\tilde{n_+}} p(\tilde{n_+}, t_s|n'_+) P_+^{ss}(n'_+) \\ &= \int_0^\infty dt_s g(t_s) \sum_{n'_+} \sum_{\tilde{n_+}} (q - qp_r + p_r)^{\tilde{n_+}} \, p(\tilde{n_+}, t_s|n'_+) P_+^{ss}(n'_+) \end{aligned}$$

Doing summation over $\tilde{n_+}$ and using the definition of the generating function F (from Eq. (2)), we get

$$F_+(q) = \int_0^\infty dt_s g(t_s) \sum_{n'_+} F((q - qp_r + p_r), t_s|n'_+) P_+^{ss}(n'_+)$$

Defining $h(q) = (q - qp_r + p_r)$ and using Eq. (4) for the explicit form of function F:

$$\begin{aligned} F_+(q) &= \int_0^\infty dt_s g(t_s) \sum_{n'_+} h^M \left[1 - \frac{h-1}{h} e^{-kt_s}\right]^{M-n'_+} P_+^{ss}(n'_+) \\ &= \int_0^\infty dt_s g(t_s) \left[h - (h-1)e^{-kt_s}\right]^M \sum_{n'_+} \left(\frac{h}{h-(h-1)e^{-kt_s}}\right)^{n'_+} P_+^{ss}(n'_+) \\ &= \int_0^\infty dt_s g(t_s) \left[h - (h-1)e^{-kt_s}\right]^M F_+\left[\frac{h}{h-(h-1)e^{-kt_s}}\right] \\ &= \int_0^\infty dt_s g(t_s) \left[h(1-e^{-kt_s}) + e^{-kt_s}\right]^M F_+\left[\frac{h}{h(1-e^{-kt_s}) + e^{-kt_s}}\right] \end{aligned} \tag{14}$$

In the above we have used the definition of F_+ from Eq(11). In Eq. (14) we have

a self-consistent integral equation for the function F_+ with two different arguments, and involving an integration over the inter-spike interval t_s. Clearly, it is difficult to solve the equation directly for $F_+(q)$. But as we show below, $F_+(q)$ may be obtained as a series expansion around $q = 1$, that is

$$F_+(q) = \sum_{n=0}^{\infty} \frac{(q-1)^n}{n!} F_+^{(n)}(1) \tag{15}$$

where the series coefficients $F_+^{(n)}(1) = \left.\frac{\partial^n F_+(q)}{\partial q^n}\right|_{q=1}$. The procedure of obtaining these coefficients are as follows.

Taking derivative with respect to q on both side of Eq. (14), we have

$$\begin{aligned}\frac{\partial F_+(q)}{\partial q} =& \frac{\partial h}{\partial q} \int_0^\infty dt_s g(t_s) \left(M \left[h(1-e^{-kt_s}) + e^{-kt_s}\right]^{M-1} (1-e^{-kt_s}) F_+ \left[\frac{h}{h(1-e^{-kt_s}) + e^{-kt_s}}\right] \right. \\ & \left. + \left[h(1-e^{-kt_s}) + e^{-kt_s}\right]^M \frac{\partial F_+[\ .\ ]}{\partial[\ .\ ]} \frac{e^{-kt_s}}{(h(1-e^{-kt_s}) + e^{-kt_s})^2} \right)\end{aligned} \tag{16}$$

where $[\ .\ ]$ is a short hand for $\left[\frac{h}{h(1-e^{-kt_s})+e^{-kt_s}}\right]$. Since $\frac{\partial h}{\partial q} = (1-p_r)$, $h(q)\big|_{q=1} = 1$, $[\ .\ ]\big|_{q=1} = 1$, $F_+(1) = 1$, and $\left.\frac{\partial F_+[\ .\ ]}{\partial[\ .\ ]}\right|_{q=1} = \left.\frac{\partial F_+(q)}{\partial q}\right|_{q=1}$, we have

$$\left.\frac{\partial F_+(q)}{\partial q}\right|_{q=1} = (1-p_r) \int_0^\infty dt_s g(t_s) \left(M(1-e^{-kt_s}) + \left.\frac{\partial F_+(q)}{\partial q}\right|_{q=1} e^{-kt_s} \right) \tag{17}$$

Defining the quantities $\psi_{n,m}$ and L_n as follows,

$$\begin{aligned}\psi_{n,m} &= \int_0^\infty dt_s g(t_s) e^{-nkt_s} (e^{kt_s} - 1)^{n-m} \\ L_n =& \psi_{n,n} = \int_0^\infty dt_s g(t_s) e^{-nkt_s}\end{aligned} \tag{18}$$

we have

$$F_+^{(1)}(1) = (1-p_r) \left(M\psi_{1,0} + L_1 F_+^{(1)}(1) \right) \tag{19}$$

where we have set $\left.\frac{\partial F_+(q)}{\partial q}\right|_{q=1} = F_+^{(1)}(1)$ according to the general definition of the n-th series coefficient above.

Next we may take derivative of Eq. (16) with respect to q and set $q = 1$ and obtain an equation for $F_+^{(2)}(1)$. We find that it is linearly coupled to $F_+^{(1)}(1)$ as follows:

$$F_+^{(2)}(1) = (1-p_r)^2 \left(M(M-1)\psi_{2,0} + (M-1)\psi_{2,1}F_+^{(1)}(1) + L_2 F_+^{(2)}(1) \right). \tag{20}$$

We may follow the same procedure to obtain equations for the higher derivatives. It is clumsy to do it manually, so we use Mathematica for this. We use symbolic derivatives of Eq. (16) and automatic replacement of terms by the ψ functions using the *Replace* syntax. The result are the equations for the next two series coefficients.

$$\begin{aligned} F_+^{(3)}(1) =& (1-p_r)^3 \Big(M(M-1)(M-2)\psi_{3,0} + (M-1)(M-2)\psi_{3,1}F_+^{(1)}(1) \\ &+ (M-2)\psi_{3,2}F_+^{(2)}(1) + L_3 F_+^{(3)}(1) \Big) \end{aligned} \tag{21}$$

$$\begin{aligned} F_+^{(4)}(1) =& (1-p_r)^4 \Big(M(M-1)(M-2)(M-3)\psi_{4,0} + (M-1)(M-2)(M-3)\psi_{4,1}F_+^{(1)}(1) \\ &+ (M-2)(M-3)\psi_{4,2}F_+^{(2)}(1) + (M-3)\psi_{4,3}F_+^{(3)}(1) + L_4 F_+^{(4)}(1) \Big) \end{aligned} \tag{22}$$

Eqs. (19) - (22) relate the four derivates $F_+^{(1)}(1), F_+^{(2)}(1), F_+^{(3)}(1)$ and $F_+^{(4)}(1)$ linearly. So, it is easy to obtain solutions by inverting a 4×4 matrix, using Mathematica. The explicit expressions of the four coefficients are

$$F_+^{(1)}(1) = \frac{(1-p_r)M\psi_{1,0}}{1-(1-p_r)L_1} \tag{23}$$

$$F_+^{(2)}(1) = \frac{(1-p_r)^2 M(M-1)}{1-(1-p_r)^2 L_2} \left[\psi_{2,0} + \frac{2(1-p_r)\psi_{2,1}\psi_{1,0}}{1-(1-p_r)L_1} \right] \tag{24}$$

$$\begin{aligned} F_+^{(3)}(1) =& \frac{(1-p_r)^3 M(M-1)(M-2)}{1-(1-p_r)^3 L_3} \Bigg[\psi_{3,0} + \frac{3(1-p_r)\psi_{3,1}\psi_{1,0}}{1-(1-p_r)L_1} \\ &+ \frac{3(1-p_r)^2\psi_{3,2}\psi_{2,0}}{1-(1-p_r)^2 L_2} + \frac{6(1-p_r)^3\psi_{3,2}\psi_{2,1}\psi_{1,0}}{(1-(1-p_r)L_1)(1-(1-p_r)^2 L_2)} \Bigg] \end{aligned} \tag{25}$$

$$\begin{aligned} F_+^{(4)}(1) =& \frac{(1-p_r)^4 M(M-1)(M-2)(M-3)}{1-(1-p_r)^4 L_4} \Bigg[\psi_{4,0} + \frac{4(1-p_r)\psi_{4,1}\psi_{1,0}}{1-(1-p_r)L_1} \\ &+ \frac{4(1-p_r)^3\psi_{4,3}\psi_{3,0}}{1-(1-p_r)^3 L_3} + \frac{6(1-p_r)^2\psi_{4,2}\psi_{2,0}}{1-(1-p_r)^2 L_2} + \frac{12(1-p_r)^3\psi_{4,2}\psi_{2,1}\psi_{1,0}}{(1-(1-p_r)L_1)(1-(1-p_r)^2 L_2)} \end{aligned}$$

$$+\frac{12(1-p_r)^4\psi_{4,3}\psi_{3,1}\psi_{1,0}}{(1-(1-p_r)L_1)(1-(1-p_r)^3L_3)}+\frac{12(1-p_r)^5\psi_{4,3}\psi_{3,2}\psi_{2,0}}{(1-(1-p_r)^2L_2)(1-(1-p_r)^3L_3)}$$
$$+\frac{24(1-p_r)^6\psi_{4,3}\psi_{3,2}\psi_{2,1}\psi_{1,0}}{(1-(1-p_r)L_1)(1-(1-p_r)^2L_2)(1-(1-p_r)^3L_3)}\Bigg] \tag{26}$$

In the above expressions, Eqs. (23) - (26), we notice the following patterns. The terms outside the square brackets are of the form $\binom{M}{n}n!\frac{(1-p_r)^n}{1-(1-p_r)^nL_n}$ for the n-th coefficient. Except for the first term, the denominators of the terms inside the square brackets for the n-th coefficient involve factors $(1-(1-p_r)^jL_j)$ with $j \neq n$ or 0. The most crucial fact is that each such term may be associated with a set of integers which are subsets of the set of integers $\{1, 2, \cdots, n-1\}$. For example, a subset of $z \leq (n-1)$ positive integer elements is $S_{(n-1)} = (m_z, m_{z-1}, \cdots, m_1) = \{m_i\}$ with $i = z, z-1, \cdots, 1$, and every $m_i \in \{1, 2, \cdots, n-1\}$ and $m_z > m_{z-1} > \cdots m_1$. The power of $(1-p_r)$ in the numerator of each term is equal to $\sum_{i=1}^{z} m_i$. The subscript of ψ factors are formed by pairs of successive integers drawn from the ordered array of numbers: $n, m_z, m_{z-1}, \cdots, m_1, 0$. The numeric factors in any numerator can be absorbed into the ψ factors by introducing the quantities $\phi_{n,m} = \binom{n}{m}\psi_{n,m}$. Putting together all these observations of the patterns, we may write down a general form of $F_+^{(n)}(1)$ as follows:

$$F_+^{(n)}(1) = \binom{M}{n}n!\frac{(1-p_r)^n}{1-(1-p_r)^nL_n}\left[\phi_{n,0} + \sum_{\{S_{(n-1)}\}}\frac{(1-p_r)^{\sum_i m_i}\phi_{n,m_z}\phi_{m_z,m_{z-1}}\cdots\phi_{m_1,0}}{\prod_i(1-(1-p_r)^{m_i}L_{m_i})}\right] \tag{27}$$

where the sum over $\{S_{(n-1)}\}$ runs over all such subsets as $S_{(n-1)}$ mentioned above.

Using Eq. (27) in Eq. (15), we can finally write down the expression of $F_+(q)$ as a series expansion around $q = 1$,

$$\boxed{F_+(q) = \sum_{n=0}^{\infty}(q-1)^n\binom{M}{n}\frac{(1-p_r)^n}{1-(1-p_r)^nL_n}\left[\phi_{n,0} + \sum_{\{S_{(n-1)}\}}\frac{(1-p_r)^{\sum_i m_i}\phi_{n,m_z}\phi_{m_z,m_{z-1}}\cdots\phi_{m_1,0}}{\prod_i(1-(1-p_r)^{m_i}L_{m_i})}\right]} \tag{28}$$

4 Relations between the generating functions, and the quantal content distribution $Q^{ss}(b)$

Let us denote the probability distribution of having n_- number of docked vesicles before an AP in the steady state by $P_-^{ss}(n_-)$. It is easy to see from similar arguments as in Section 2, that $P_-^{ss}(n_-)$ will be related to the three distributions: $P_+^{ss}(n_+)$ (to have an initial number), $p(n_-|t_s, n_+)$ (for docked vesicles to build up), and $g(t_s)$ (for AP to appear). Thus

$$P_-^{ss}(n_-) = \sum_{n_+} \int_0^\infty p(n_-, t_s|n_+) P_+^{ss}(n_+) g(t_s) dt_s \tag{29}$$

We define its generating function as

$$F_-(q) = \sum_{n_-=0}^{\infty} q^{n_-} P_-^{ss}(n_-) \tag{30}$$

The ultimate object of our interest, namely the distribution of quantal content b in the steady state, is related to the distribution $P_-^{ss}(n_-)$ as:

$$Q^{ss}(b) = \sum_{n_-} P_-^{ss}(n_-) B(n_-, p_r, b) \tag{31}$$

Note that the the crucial fact is that we are averaging the well-known binomial distribution now, over the stochastically generated docked vesicle number n_- just prior to an action potential. As we would see, the resultant averaged distribution would be different from the original binomial. The generating function corresponding to $Q^{ss}(b)$ is defined as

$$F_b(q) = \sum_{b=0}^{\infty} q^b Q^{ss}(b) \tag{32}$$

We have four distributions $p(n_-, t_s|n_+)$, $P_+^{ss}(n_+)$, $P_-^{ss}(n_-)$, and $Q^{ss}(b)$ and four corresponding generating functions F, F_+, F_- and F_b, respectively. Of these, we have already calculated F (Eq. (4)) and F_+ (Eq. (28)). We would now proceed to relate the generating functions F_- and F_b to F_+. Once F_b is known explicitly using the

expression of F_+, we would then obtain $Q^{ss}(b)$ by taking suitable derivatives of $F_b(q)$ with respect to q.

Using Eq. (29) in Eq. (30) we get,

$$\begin{aligned} F_-(q) &= \sum_{n_-} q^{n-} \left(\sum_{n_+} \int_0^\infty p\left(n_-, t_s | n_+\right) P_+^{ss}\left(n_+\right) g(t_s) dt_s \right) \\ &= \int_0^\infty g(t_s) dt_s \left\{ \sum_{n_+} P_+^{ss}\left(n_+\right) \sum_{n_-} p\left(n_-, t_s | n_+\right) q^{n-} \right\} \\ &= \int_0^\infty g(t_s) dt_s \left\{ \sum_{n_+} P_+^{ss}\left(n_+\right) F\left(q, t_s | n_+\right) \right\} \end{aligned}$$

In the above we have used the definition of the function F. Substituting the explicit form of $F(q, t_s|n_+)$ from Eq. (4), we have

$$\begin{aligned} F_-(q) &= \int_0^\infty g(t_s) dt_s \left\{ \sum_{n+} P_+^{ss}\left(n_+\right) q^M \left[1 + \frac{1-q}{q} e^{-kt_s} \right]^{M-n_+} \right\} \\ &= \int_0^\infty g(t_s) dt_s \left\{ \left[q + (1-q) e^{-kt_s} \right]^M F_+ \left(\frac{1}{1 + \frac{1-q}{q} e^{-kt_s}} \right) \right\} \end{aligned} \tag{33}$$

In the above we have used the definition of F_+.

Substituting $\frac{q-p_r}{1-p_r}$ in place of q in Eq. (14), and noticing $h\left(\frac{q-p_r}{1-p_r}\right) = q$, we get

$$F_+ \left(\frac{q-p_r}{1-p_r} \right) = \int_0^\infty g(t_s) dt_s \left\{ \left[q + (1-q) e^{-kt_s} \right]^M F_+ \left(\frac{1}{1 + \frac{1-q}{q} e^{-kt_s}} \right) \right\} \tag{34}$$

Comparing Eqs. (33) and (34), we immediately get,

$$F_-(q) = F_+ \left(\frac{q-p_r}{1-p_r} \right) \tag{35}$$

Substituting Eq. (31) in Eq. (32) with the binomial distribution $B(n_-, p_r, b)$ written explicitly, we have

$$F_b(q) = \sum_b q^b \left(\sum_{n_-} P_-^{ss}(n_-) \binom{n_-}{b} p_r^b \left(1-p_r\right)^{n_- - b} \right)$$

$$
\begin{aligned}
&= \sum_{n_-} P_-^{ss}(n_-)\left(qp_r + (1-p_r)\right)^{n_-} \\
&= F_-\left(qp_r + 1 - p_r\right) \\
&= F_+\left(\frac{p_r(q-1)}{1-p_r} + 1\right)
\end{aligned} \tag{36}
$$

Here we have used the definition of the function F_-, and the relation of F_+ to F_- from Eq. (35). Using the explicit form of F_+ from Eq. (28), the Eq. (36) gives,

$$
F_b(q) = \sum_{n=0}^{\infty}(q-1)^n \binom{M}{n} \frac{p_r^n}{1-(1-p_r)^n L_n}\left[\phi_{n,0} + \sum_{\{S_{(n-1)}\}} \frac{(1-p_r)^{\sum_i m_i}\phi_{n,m_z}\phi_{m_z,m_{z-1}}\cdots\phi_{m_1,0}}{\prod_i (1-(1-p_r)^{m_i}L_{m_i})}\right] \tag{37}
$$

We may invert Eq. (32), to obtain the quantal content distribution $Q^{ss}(b)$ from successive derivatives of $F_b(q)$ as follows:

$$
Q^{ss}(b) = \frac{1}{b!}\frac{\partial^b F_b(q)}{\partial q^b}\bigg|_{q=0} \tag{38}
$$

Note that q is present in $F_b(q)$ only through the factor $(q-1)^n$ in Eq. (37). Using the identity $\frac{\partial^b (q-1)^n}{\partial q^b}\Big|_{q=0} = \frac{n!}{(n-b)!}(-1)^{n-b}$, we obtain our final desired result

$$
\boxed{Q^{ss}(b) = \sum_{n=0}^{\infty}\binom{n}{b}(-1)^{n-b}\binom{M}{n}\frac{p_r^n}{1-(1-p_r)^n L_n}\left[\phi_{n,0} + \sum_{\{S_{(n-1)}\}} \frac{(1-p_r)^{\sum_i m_i}\phi_{n,m_z}\phi_{m_z,m_{z-1}}\cdots\phi_{m_1,0}}{\prod_i (1-(1-p_r)^{m_i}L_{m_i})}\right]} \tag{39}
$$

Moments:

(i) For the general distribution of ISIs, following Eq. (39), the mean quantal content $\langle b\rangle$ is given by

$$
\langle b\rangle = \sum_{b=0}^{M} bQ^{ss}(b)
$$

$$
\begin{aligned}
&= \sum_{n=0}^{M} \left[\sum_{b=0}^{n} (-1)^b b \binom{n}{b} \right] (-1)^n \binom{M}{n} \frac{p_r^n}{1-(1-p_r)^n L_n} \\
&\quad \times \left[\phi_{n,0} + \sum_{\{S_{(n-1)}\}} \frac{(1-p_r)^{\sum_i m_i} \phi_{n,m_z} \phi_{m_z,m_{z-1}} \cdots \phi_{m_1,0}}{\prod_i (1-(1-p_r)^{m_i} L_{m_i})} \right]
\end{aligned} \tag{40}
$$

Note that

$$
\begin{aligned}
\sum_{b=0}^{n} (-1)^b b \binom{n}{b} &= x \frac{\partial}{\partial x} \left[\sum_{b=0}^{n} \binom{n}{b} x^b \right] \Bigg|_{x=-1} \\
&= x \frac{\partial}{\partial x} (1+x)^n \Bigg|_{x=-1} = xn(1+x)^{n-1} \Bigg|_{x=-1} = -\delta_{n,1}
\end{aligned} \tag{41}
$$

Substituting Eq. (41) in Eq. (40), we have

$$
\begin{aligned}
\langle b \rangle &= -\sum_{n=0}^{M} \delta_{n,1} (-1)^n \binom{M}{n} \frac{p_r^n}{1-(1-p_r)^n L_n} \left[\phi_{n,0} + \sum_{\{S_{(n-1)}\}} \frac{(1-p_r)^{\sum_i m_i} \phi_{n,m_z} \phi_{m_z,m_{z-1}} \cdots \phi_{m_1,0}}{\prod_i (1-(1-p_r)^{m_i} L_{m_i})} \right] \\
&= \frac{M p_r \phi_{1,0}}{1-(1-p_r) L_1}
\end{aligned} \tag{42}
$$

(ii) Similarly, the second moment $\langle b^2 \rangle$ is given as:

$$
\begin{aligned}
\langle b^2 \rangle &= \sum_{b=0}^{M} b^2 Q^{ss}(b) \\
&= \sum_{n=0}^{M} \left[\sum_{b=0}^{n} (-1)^b b^2 \binom{n}{b} \right] (-1)^n \binom{M}{n} \frac{p_r^n}{1-(1-p_r)^n L_n} \\
&\quad \times \left[\phi_{n,0} + \sum_{\{S_{(n-1)}\}} \frac{(1-p_r)^{\sum_i m_i} \phi_{n,m_z} \phi_{m_z,m_{z-1}} \cdots \phi_{m_1,0}}{\prod_i (1-(1-p_r)^{m_i} L_{m_i})} \right]
\end{aligned} \tag{43}
$$

Where,

$$
\sum_{b=0}^{n} (-1)^b b^2 \binom{n}{b} = x^2 \frac{\partial^2}{\partial x^2} \left[\sum_{b=0}^{n} \binom{n}{b} x^b \right] \Bigg|_{x=-1} + x \frac{\partial}{\partial x} \left[\sum_{b=0}^{n} \binom{n}{b} x^b \right] \Bigg|_{x=-1}
$$

$$
\begin{aligned}
&= x^2 n(n-1)(1+x)^{n-2}\Big|_{x=-1} - \delta_{n,1} \\
&= 2\delta_{n,2} - \delta_{n,1}
\end{aligned} \tag{44}
$$

Substituting Eq. (44) in Eq. (43), we have

$$
\begin{aligned}
\langle b^2 \rangle =& \sum_{n=0}^{M} \left[2\delta_{n,2} - \delta_{n,1}\right] (-1)^n \binom{M}{n} \frac{p_r^n}{1-(1-p_r)^n L_n} \\
&\times \left[\phi_{n,0} + \sum_{\{S_{(n-1)}\}} \frac{(1-p_r)^{\sum_i m_i} \phi_{n,m_z} \phi_{m_z,m_{z-1}} \cdots \phi_{m_1,0}}{\prod_i (1-(1-p_r)^{m_i} L_{m_i})} \right] \\
=& \frac{M(M-1)p_r^2}{1-(1-p_r)^2 L_2} \left[\phi_{2,0} + \frac{(1-p_r)\phi_{2,1}\phi_{1,0}}{1-(1-p_r)L_1} \right] + \frac{M p_r \phi_{1,0}}{1-(1-p_r)L_1}
\end{aligned} \tag{45}
$$

Using Eqs. (42) and (45), CV^2 can be easily obtained as

$$
\begin{aligned}
CV^2 =& \frac{\langle b^2 \rangle}{\langle b \rangle^2} - 1 \\
=& \left(\frac{1-(1-p_r)L_1}{M p_r \phi_{1,0}} \right)^2 \frac{M(M-1)p_r^2}{1-(1-p_r)^2 L_2} \left[\phi_{2,0} + \frac{(1-p_r)\phi_{2,1}\phi_{1,0}}{1-(1-p_r)L_1} \right] \\
&+ \frac{1-(1-p_r)L_1}{M p_r \phi_{1,0}} - 1
\end{aligned}
$$

Note that $1 - L_1 = \phi_{1,0}$. So, we have

$$
\begin{aligned}
CV^2 =& \left(\frac{\phi_{1,0} + p_r L_1}{M p_r \phi_{1,0}} \right)^2 \frac{M(M-1)p_r^2}{1-(1-p_r)^2 L_2} \left[\phi_{2,0} + \frac{(1-p_r)\phi_{2,1}\phi_{1,0}}{\phi_{1,0} + p_r L_1} \right] \\
&+ \frac{\phi_{1,0} + p_r L_1}{M p_r \phi_{1,0}} - 1 \\
=& \frac{\phi_{1,0} + p_r L_1}{M \phi_{1,0}} \left[\frac{(M-1)}{1-(1-p_r)^2 L_2} \left[\phi_{2,0} \left(1 + \frac{p_r L_1}{\phi_{1,0}} \right) + (1-p_r)\phi_{2,1} \right] + \frac{1}{p_r} \right] - 1
\end{aligned} \tag{46}
$$

5 The distribution $Q^{ss}(b)$ for two special cases of inter AP interval distribution $g(t_s)$

(a) The deterministic case – APs at a fixed frequency $f = 1/T$

Assuming the APs arrive after fixed time duration T, the corresponding distribution $g(t_s) = \delta(t_s - T)$. This is most often the pattern of input spike train used by experimentalists to excite neuronal response at a fixed frequency $f = 1/T$. We may calculate using Eq. (18),

$$\begin{aligned}
\psi_{n,m} &= \int_0^\infty dt_s \delta(t_s - T) e^{-nkt_s}(e^{kt_s} - 1)^{n-m} = e^{-nkT}(e^{kT} - 1)^{n-m}, \\
L_n &= \psi_{n,n} = e^{-nkT}, \\
\psi_{n,m_z}\psi_{m_z,m_{z-1}}\cdots\psi_{m_1,0} &= e^{-nkT}(e^{kT} - 1)^n e^{-kT\sum_{i=1}^z m_i} = (1 - e^{-kT})^n e^{-kT\sum_{i=1}^z m_i}
\end{aligned} \tag{47}$$

Substituting these expressions in the Eq. (39), and recalling $\phi_{n,m} = \binom{n}{m}\psi_{n,m}$, we have

$$\begin{aligned}
Q^{ss}(b) &= \sum_{n=0}^\infty \binom{n}{b}(-1)^{n-b}\binom{M}{n}\frac{p_r^n}{1-(1-p_r)^n L_n}\left[\phi_{n,0} + \sum_{\{S_{(n-1)}\}} \frac{(1-p_r)^{\sum_i m_i}\phi_{n,m_z}\phi_{m_z,m_{z-1}}\cdots\phi_{m_1,0}}{\prod_i (1-(1-p_r)^{m_i}L_{m_i})}\right] \\
&= \sum_{n=0}^\infty \binom{n}{b}(-1)^{n-b}\binom{M}{n}\frac{p_r^n}{1-(e^{-kT}(1-p_r))^n}(1-e^{-kT})^n \\
&\qquad \left[1 + \sum_{\{S_{(n-1)}\}}\binom{n}{m_z}\binom{m_z}{m_{z-1}}\cdots\binom{m_2}{m_1}\prod_i \frac{(e^{-kT}(1-p_r))^{m_i}}{(1-(e^{-kT}(1-p_r))^{m_i})}\right]
\end{aligned} \tag{48}$$

It is important to remind that $\{S_{(n-1)}\}$ is the set of all the subsets of the set $\{1, 2, \cdots, n-1\}$. To proceed further, we need to use the following identity (for

$|x| < 1$) – for proof see Section 6:

$$1 + \sum_{\{S_{(n-1)}\}} \binom{n}{m_z}\binom{m_z}{m_{z-1}}\cdots\binom{m_2}{m_1}\prod_i \frac{x^{m_i}}{(1-x^{m_i})} = \frac{1-x^n}{(1-x)^n} \tag{49}$$

Using the identity (Eq. (49)) in Eq. (48), the expression simplifies to give,

$$\begin{aligned}
Q^{ss}(b) &= \sum_{n=0}^{\infty}\binom{n}{b}(-1)^{n-b}\binom{M}{n}\frac{p_r^n}{1-(e^{-kT}(1-p_r))^n}(1-e^{-kT})^n\frac{1-(e^{-kT}(1-p_r))^n}{(1-e^{-kT}(1-p_r))^n}\\
&= \sum_{n=0}^{\infty}\binom{n}{b}(-1)^{n-b}\binom{M}{n}\frac{p_r^n}{(1-e^{-kT}(1-p_r))^n}(1-e^{-kT})^n\\
&= \sum_{n=0}^{\infty}\binom{n}{b}(-1)^{b}\binom{M}{n}\left(\frac{-p_r(1-e^{-kT})}{1-e^{-kT}(1-p_r)}\right)^n
\end{aligned}$$

Further using the identity, $\sum_{n=b}^{M} x^n\binom{n}{b}\binom{M}{n} = \binom{M}{b}x^b(x+1)^{M-b}$ we finally get

$$\boxed{Q^{ss}(b) = \binom{M}{b}\left(\frac{(1-e^{-kT})p_r}{1-(1-p_r)e^{-kT}}\right)^b\left(1-\frac{(1-e^{-kT})p_r}{1-(1-p_r)e^{-kT}}\right)^{M-b} = B(M, p_{rb}, b)} \tag{50}$$

Hence, the steady state quantal content distribution for the deterministic $g(t_s)$ is still a binomial distribution, but with the parameters M (maximal docked vesicle number) and an effective release probability p_{rb} (different from p_r) given by:

$$p_{rb} = \frac{(1-e^{-kT})p_r}{1-(1-p_r)e^{-kT}} \tag{51}$$

In order to compare the exact distribution (Eq. (50)) with the approximate binomial distribution $B(\langle n_-\rangle, p_r, b)$ where $\langle n_-\rangle$ is the mean number of docked vesicles just before the AP spikes, we need to calculate an expression for $\langle n_-\rangle$. It is easy to calculate $\langle n_-\rangle$ from the generating function $F_-(q)$ as $\langle n_-\rangle = \left.\frac{\partial F_-(q)}{\partial q}\right|_{q=1}$.

Taking derivative of Eq. (35) and setting $q = 1$, we get

$$\left.\frac{\partial F_-(q)}{\partial q}\right|_{q=1} = \left.\frac{\partial F_+(q)}{\partial q}\right|_{q=1}\frac{1}{(1-p_r)} \tag{52}$$

If we take the derivative of Eq. (28) with respect to q at $q = 1$, only $n = 1$ term in the summation survives. Eq. (52) will become

$$\left.\frac{\partial F_-(q)}{\partial q}\right|_{q=1} = \frac{M(1-p_r)}{1-(1-p_r)L_1}\phi_{1,0}\frac{1}{(1-p_r)}$$

Substituting the forms of L_1 and $\phi_{1,0}$ from Eq. (47), we get

$$\left.\frac{\partial F_-(q)}{\partial q}\right|_{q=1} = \frac{M(1-p_r)}{1-(1-p_r)e^{-kT}}(1-e^{-kT})\frac{1}{(1-p_r)}$$

Hence,

$$\boxed{\langle n_- \rangle = \frac{M(1-e^{-kT})}{1-(1-p_r)e^{-kT}} = M\frac{p_{rb}}{p_r}} \tag{53}$$

In the above we have used the expression of p_{rb} from Eq. (51). The Eq. (53) implies that the mean $\langle b \rangle$ of the exact binomial and the approximate binomial are equal, i.e. $Mp_{rb} = \langle n_- \rangle p_r$. But the variance of the exact distribution is $Mp_{rb}(1-p_{rb})$, different from that of the approximate binomial $\langle n_- \rangle p_r(1-p_r)$.

(b) Poisson distributed AP arrival times

APs may arrive at intervals which may be noisy. A simple way to incorporate stochasticity in the input spike train is to assume that they arrive at time intervals which are exponentially distributed with $g(t_s) = f_0 e^{-f_0 t_s}$. Note that the mean as well as characteristic spike interval is $1/f_0$. In this case using Eq. (18),

$$\begin{aligned}
\psi_{n,m} &= \int_0^\infty dt_s g(t_s) e^{-mkt_s}(1-e^{-kt_s})^{n-m} \\
&= \int_0^\infty dt_s f_0 e^{-(mk+f_0)t_s}(1-e^{-kt_s})^{n-m} \\
&= \frac{f_0}{k}\int_0^1 dz z^{\frac{mk+f_0}{k}-1}(1-z)^{n-m} \\
&= \frac{f_0}{k}B\left(m+\frac{f_0}{k}, n-m+1\right) = \frac{f_0}{k}\frac{\Gamma(-m+n+1)\Gamma\left(\frac{f_0}{k}+m\right)}{\Gamma\left(\frac{f_0}{k}+n+1\right)},
\end{aligned} \tag{54}$$

where we have used Beta function $B(a,b) = \Gamma(a)\Gamma(b)/\Gamma(a+b)$, and then

$$L_n = \psi_{n,n} = \frac{f_0}{k}\frac{\Gamma(1)\Gamma\left(\frac{f_0}{k}+n\right)}{\Gamma\left(\frac{f_0}{k}+n+1\right)} = \frac{f_0}{f_0+nk}. \tag{55}$$

Moreover using Eq. (54), we have

$$\phi_{n,m} = \binom{n}{m}\psi_{n,m} = \binom{n}{m}\frac{f_0}{k}\frac{\Gamma(-m+n+1)\Gamma\left(\frac{f_0}{k}+m\right)}{\Gamma\left(\frac{f_0}{k}+n+1\right)} = \frac{f_0}{k}\frac{\Gamma(n+1)\Gamma\left(\frac{f_0}{k}+m\right)}{\Gamma(m+1)\Gamma\left(\frac{f_0}{k}+n+1\right)} \tag{56}$$

$$\begin{aligned}\Rightarrow \phi_{n,m}\phi_{m,l} =& \frac{f_0^2}{k^2}\frac{\Gamma(n+1)\Gamma\left(\frac{f_0}{k}+m\right)}{\Gamma(m+1)\Gamma\left(\frac{f_0}{k}+n+1\right)}\frac{\Gamma(m+1)\Gamma\left(\frac{f_0}{k}+l\right)}{\Gamma(l+1)\Gamma\left(\frac{f_0}{k}+m+1\right)} \\ =& \frac{f_0^2}{k^2}\frac{k\Gamma(n+1)\Gamma\left(\frac{f_0}{k}+l\right)}{\Gamma(l+1)(f_0+km)\Gamma\left(\frac{f_0}{k}+n+1\right)}\end{aligned} \tag{57}$$

The above Eq. (57) may be extended to get the following product:

$$\phi_{n,m_z}\phi_{m_z,m_{z-1}}\cdots\phi_{m_1,0} = \frac{f_0^{z+1}}{k^{z+1}}\frac{n!\Gamma\left(\frac{f_0}{k}\right)}{\Gamma\left(\frac{f_0}{k}+n+1\right)}\prod_i \frac{k}{f_0+km_i} \tag{58}$$

Substituting Eq. (58) into Eq. (39), we have

$$\begin{aligned}Q^{ss}(b) =& \sum_{n=0}^{\infty}\binom{n}{b}(-1)^{n-b}\binom{M}{n}\frac{p_r^n}{1-(1-p_r)^n L_n}\left[\phi_{n,0} + \sum_{\{S_{(n-1)}\}}\frac{(1-p_r)^{\sum_i m_i}\frac{f_0^{z+1}}{k^{z+1}}\frac{n!\Gamma\left(\frac{f_0}{k}\right)}{\Gamma\left(\frac{f_0}{k}+n+1\right)}\prod_i\frac{k}{f_0+km_i}}{\prod_i(1-(1-p_r)^{m_i}L_{m_i})}\right] \\ =& \sum_{n=0}^{\infty}\binom{n}{b}(-1)^{n-b}\binom{M}{n}\frac{p_r^n}{1-(1-p_r)^n L_n}\frac{n!\Gamma\left(\frac{f_0}{k}\right)}{\Gamma\left(\frac{f_0}{k}+n+1\right)}\frac{f_0}{k}\left[1 + \sum_{\{S_{(n-1)}\}}\frac{(1-p_r)^{\sum_i m_i}\prod_i\frac{f_0}{f_0+km_i}}{\prod_i(1-(1-p_r)^{m_i}L_{m_i})}\right]\end{aligned}$$

From Eq. (55), substituting $\frac{f_0}{f_0+km_i} = L_{m_i}$, we have

$$Q^{ss}(b) = \sum_{n=0}^{\infty}\binom{n}{b}(-1)^{n-b}\binom{M}{n}\frac{p_r^n}{1-(1-p_r)^n L_n}\frac{n!\Gamma\left(\frac{f_0}{k}+1\right)}{\Gamma\left(\frac{f_0}{k}+n+1\right)}\left[1 + \sum_{\{S_{(n-1)}\}}\prod_i\frac{(1-p_r)^{m_i}L_{m_i}}{(1-(1-p_r)^{m_i}L_{m_i})}\right] \tag{59}$$

We may simplify the expression above by using the following identity valid for any

arbitrary function f – for proof see Section 7:

$$1+\sum_{\{S_{(n-1)}\}}\prod_i \frac{f(m_i)}{1-f(m_i)} = \frac{1}{\prod_{i=1}^{n-1}(1-f(i))} \tag{60}$$

Using Eq. (60) in Eq. (59), we get

$$Q^{ss} = \sum_{n=0}^{\infty}\binom{n}{b}(-1)^{n-b}\binom{M}{n}\frac{p_r^n n!\Gamma\left(\frac{f_0}{k}+1\right)}{(1-(1-p_r)^n L_n)\Gamma\left(\frac{f_0}{k}+n+1\right)}\frac{1}{\prod_{i=1}^{n-1}(1-(1-p_r)^i L_i)}$$

Substituting back $L_i = \frac{f_0}{f_0+ki}$, we have

$$Q^{ss} = \sum_{n=0}^{\infty}\binom{n}{b}(-1)^{n-b}\binom{M}{n}\frac{p_r^n n!\Gamma\left(\frac{f_0}{k}+1\right)}{\Gamma\left(\frac{f_0}{k}+n+1\right)}\frac{1}{\prod_{i=1}^{n}\frac{(f_0+ki-(1-p_r)^i f_0)}{f_0+ki}}$$

$$\boxed{Q^{ss}(b) = \sum_{n=0}^{\infty}(-1)^{n-b}\binom{n}{b}\binom{M}{n}\frac{n!(kp_r)^n}{\prod_{i=1}^{n}(f_0+ki-(1-p_r)^i f_0)}} \tag{61}$$

Thus the steady state quantal content distribution for the spike intervals drawn from a Poisson processes is not a Binomial, but instead the above distribution in Eq. (61).

Moments:

(i) For the exponentially distributed ISIs, the mean quantal content $\langle b\rangle$ can be obtained by substituting $\phi_{1,0} = \frac{k}{f_0+k}$ and $L_1 = \frac{f_0}{f_0+k}$ from Eqs. (56) and (55) respectively, into the general $\langle b\rangle$ expression (Eq. (42)) as follows

$$\begin{aligned}\langle b\rangle =& \frac{Mp_r\frac{k}{f_0+k}}{1-(1-p_r)\frac{f_0}{f_0+k}}\\ =& \frac{Mkp_r}{k+f_0p_r}\end{aligned} \tag{62}$$

(ii) Similarly, the CV^2 can be obtained by substituting the expressions: $\phi_{1,0} = \frac{k}{f_0+k}$, $\phi_{2,0} = \frac{2k^2}{(f_0+k)(f_0+2k)}$, $\phi_{2,1} = \frac{2f_0k}{(f_0+k)(f_0+2k)}$, $L_1 = \frac{f_0}{f_0+k}$, and $L_2 = \frac{f_0}{f_0+2k}$ from Eqs. (56) and (55), into the general CV^2 expression (Eq. (46)) as follows

$$\begin{aligned} CV^2 =& \frac{k+f_0p_r}{Mk}\left[\frac{(M-1)(f_0+2k)}{f_0+2k-(1-p_r)^2f_0}\left(\frac{(k+f_0p_r)2k^2+2(1-p_r)f_0k^2}{k\left(f_0+k\right)\left(f_0+2k\right)}\right)+\frac{1}{p_r}\right]-1 \\ =& \frac{k+f_0p_r}{Mk}\left[\frac{(M-1)(f_0+2k)}{f_0+2k-(1-p_r)^2f_0}\left(\frac{2k^2(f_0+k)}{k\left(f_0+k\right)\left(f_0+2k\right)}\right)+\frac{1}{p_r}\right]-1 \\ =& \frac{1}{M}\left(\frac{2(M-1)\left(k+f_0p_r\right)}{2k+f_0p_r\left(2-p_r\right)}+\frac{f_0}{k}-M+\frac{1}{p_r}\right) \end{aligned} \tag{63}$$

6 Proof of the identity in Eq. (49):

The identity can be proved using the principle of strong mathematical induction as follows.

We first verify the identity for $n = 1$ and 2 explicitly. For $n = 1$, LHS of Eq. (49) will be simply equal to 1 as the summation term does not contribute anything. The RHS is also equal to 1, so the identity is true for $n = 1$. For $n = 2$, $\{S_{(1)}\} = \{\{1\}\}$. So, the LHS of Eq. (49) will be equal to $1 + \binom{2}{1}\frac{x}{1-x} = \frac{1+x}{1-x} = \frac{1-x^2}{(1-x)^2} = RHS$. Hence, we have verified the identity for $n = 2$ as well.

Let us assume that the identity is true for all integer values of $n \in [1, k]$. We would then show below that it is true for $n = k + 1$. For $n = k + 1$ we have:

$$\begin{aligned} LHS =& 1+\sum_{\{S_{(k)}\}}\binom{k+1}{m_z}\binom{m_z}{m_{z-1}}\cdots\binom{m_2}{m_1}\prod_i\frac{x^{m_i}}{(1-x^{m_i})} \\ =& 1+\binom{k+1}{1}\frac{x}{1-x}+\sum_{\substack{\{S_{(k)}\}\\ m_z\neq 1}}\binom{k+1}{m_z}\binom{m_z}{m_{z-1}}\cdots\binom{m_2}{m_1}\prod_i\frac{x^{m_i}}{(1-x^{m_i})} \end{aligned} \tag{64}$$

where in the last step, we have separated out the contribution of $m_z = 1$ in the summation. The crucial step in our proof comes from the idea that the subsets in the set $\{S_{(k)}\}$ (with $m_z \neq 1$) can be clubbed into different groups, such that the largest element in all the subsets in a particular group are equal. There will be $k-1$ such groups as the maximum element m_z can range from 2 to k. With the summing

over all such groups explicitly shown, Eq. (64) becomes

$$LHS = 1+\binom{k+1}{1}\frac{x}{1-x}+\sum_{m_z=2}^{k}\binom{k+1}{m_z}\frac{x^{m_z}}{1-x^{m_z}}\left[\sum_{\{S_{(m_z-1)}\}}\binom{m_z}{m_{z-1}}\cdots\binom{m_2}{m_1}\prod_i\frac{x^{m_i}}{(1-x^{m_i})}+1\right] \tag{65}$$

Note that 1 is added manually inside the square bracket to take care of the subsets with only one element m_z, as these subsets are not taken into account by the summation term over the subsets $\{S_{(m_z-1)}\}$. The expression inside the square bracket is equal to the LHS of Eq. (49) with $n = m_z$. Note that as positive integer $m_z \leq k$, by assumption the identity Eq. (49) is true. So, substituting the form of RHS from Eq. (49) into the square bracket of Eq. (65), we have

$$\begin{aligned}
LHS =& 1+\binom{k+1}{1}\frac{x}{1-x}+\sum_{m_z=2}^{k}\binom{k+1}{m_z}\frac{x^{m_z}}{1-x^{m_z}}\left[\frac{1-x^{m_z}}{(1-x)^{m_z}}\right]\\
=& 1+\binom{k+1}{1}\frac{x}{1-x}+\sum_{m_z=2}^{k}\binom{k+1}{m_z}\left(\frac{x}{1-x}\right)^{m_z}\\
=& \sum_{m_z=0}^{k}\binom{k+1}{m_z}\left(\frac{x}{1-x}\right)^{m_z}\\
=& \sum_{m_z=0}^{k+1}\binom{k+1}{m_z}\left(\frac{x}{1-x}\right)^{m_z}-\left(\frac{x}{1-x}\right)^{k+1}\\
=& \left(\frac{1}{1-x}\right)^{k+1}-\left(\frac{x}{1-x}\right)^{k+1}\\
=& \frac{1-x^{k+1}}{(1-x)^{k+1}} = RHS
\end{aligned} \tag{66}$$

Hence, we have shown above that the identity is true for $n = k+1$. Since integer $k \geq 2$ is arbitrary, we have proved the identity in Eq. (49) using the method of strong induction.

7 Proof of the identity in Eq. (60):

Here is the proof of the identity using the method of mathematical induction:

For $n = 2$, $\{S\}$, the set of all the subsets of $\{1\}$, is simply $\{\{1\}\}$. Hence, the LHS

of Eq. (60) will be equal to

$$LHS = 1 + \prod_{\{1\}} \frac{f(m_i)}{1 - f(m_i)} = 1 + \frac{f(1)}{1 - f(1)} = \frac{1}{1 - f(1)} = RHS \tag{67}$$

Let us assume that the identity is true for an arbitrary value of $n = k$. For, $n = k + 1$, the set $\{S\}$ of all the subsets of $\{1, 2, 3, \cdots k\}$ can be divided into three disjoint subsets:

(a) the set of all the subsets of $\{1, 2, 3, \cdots k - 1\}$.

(b) the set of all the subsets in (a) with an extra element k added to each of the subsets.

(c) $\{\{k\}\}$

Clearly, the contribution of (a) in the summation term in the LHS of Eq. (60) will be equal to that for $n = k$, that is equal to $1/\prod_{i=1}^{k-1}(1 - f(i)) - 1$. On the other hand, the contribution of (b) will be equal to that of (a) multiplied by an additional factor $\frac{f(k)}{1-f(k)}$. The contribution from (c) will be simply $\frac{f(k)}{1-f(k)}$. Adding all the three contributions,

$$\begin{aligned}
LHS =& 1 + \left(\frac{1}{\prod_{i=1}^{k-1}(1 - f(i))} - 1 \right) + \left(\frac{1}{\prod_{i=1}^{k-1}(1 - f(i))} - 1 \right) \frac{f(k)}{1 - f(k)} + \frac{f(k)}{1 - f(k)} \\
=& \frac{1}{\prod_{i=1}^{k-1}(1 - f(i))} \left(1 + \frac{f(k)}{1 - f(k)} \right) \\
=& \frac{1}{\prod_{i=1}^{k}(1 - f(i))} = RHS
\end{aligned}$$

Hence, the identity is true for $n = k+1$. Thus from the principle of mathematical induction, the identity is proved for any integer $n > 1$.

8 Saturation of time dependent p_r and k, following calcium level saturation, in steady state

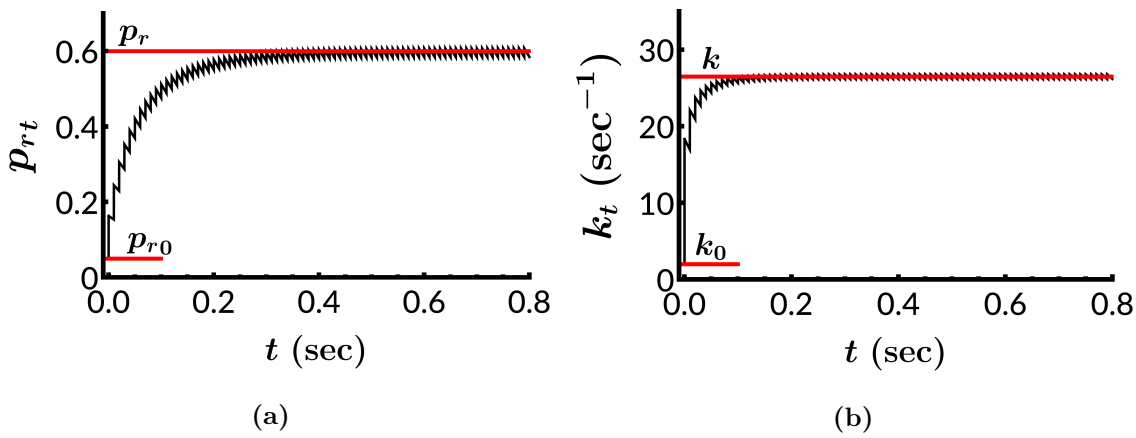

(a) (b)

Figure 1: The time-dependence of p_{rt} and k_t are shown for the parameter values given in Table 2. of Ref. [1], for parallel fiber. The initial and steady state values are marked with red lines, and the corresponding values are mentioned.

The vesicle release probability p_{rt} and the rate of docking of vesicles k_t are dependent on the time t, through their dependence on time-varying Ca^{2+} level inside the presynaptic terminal. There are different models available in the literature to describe this period of plasticity. For the purpose of demonstrating the approach to steady state, we use one such model studied in the paper by Dittman and colleagues [1]. Two different types of calcium binding targets are considered, namely F and D. The p_{rt} is related to the number CaX_F of Ca^{2+}-bound-F molecules as $p_{rt} = p_{r0} + \frac{1-p_{r0}}{\frac{K_F}{CaX_F(t)}+1}$. On the other hand, k_t is related to the number CaX_D of Ca^{2+}-bound-D sites as $k_t = k_0 + \frac{k_{\max}-k_0}{\frac{K_D}{\mathrm{ca}(t)}+1}$. Given an AP train, with m^{th} AP arriving at $t = t_m$, the dynamics of CaX_F and CaX_D are given by

$$\frac{dCaX_F}{dt} = -\frac{CaX_F}{\tau_F} + \Delta_F \sum_m \delta(t - t_m) \tag{68}$$

and,

$$\frac{dCaX_D}{dt} = -\frac{CaX_D}{\tau_D} + \Delta_D \sum_m \delta(t - t_m) \tag{69}$$

respectively. CaX_F (or CaX_D) jumps by Δ_F (or Δ_D) after each AP, and falls exponentially between two APs, with a decay constant τ_F (or τ_D). In Fig. 1, for the parameter values given in Ref. [1] for parallel fiber, we have plotted the p_{rt} and k_t as a function of t. Note that the initial values at $t \to 0$ are p_{r0} and k_0 respectively. We see that $p_{rt} \to p_r$ and $k_t \to k$ in the long time limit. This steady state limit is the focus of the entire analysis described in this paper, in which the release probability and replenishment rate has attained the steady values p_r and k respectively.

9 Kinetic Monte Carlo (KMC) code

The code used to simulate the distribution of quantal content for constant ISIs as well as Poisson train is as follows.

In [3]:

```
import math as mp
import numpy as np
```

In [ ]:

```
burst=[]

for col in range (0,100,1):
    burstt=[]
    time=[]
    M=50
    f=100
    pr =0.5
    k = 1.0
    g=1
    while g<2:
        t=0
        n=M
        nstate=[M]
        j=[]
        x=1
        ######################################################################
        #Use this part for constant ISIs

        dlist=[0]
        for i in range (100000):
            dlist.append(max(dlist)+(1/f))

        ######################################################################
        #Use this part for exponentially distributed ISIs

        dlist=[0]
        for i in range (100000):
            dlist.append(max(dlist)+(1/f)*mp.log(1/np.random.uniform(0,1)))

        ######################################################################
        while x<5000:
            p=np.random.uniform(0,1)
            for i in range (0,100,1):
                if dlist[i]<=t<=dlist[i+1] and \
                t+(1/(k*(M-n+0.000001)))*mp.log(1/p)<=dlist[i+1]:
                    n=n+1
                    t=t+(1/(k*(M-n+1+0.000001)))*mp.log(1/p)
                    time.append(t)
                    break
                elif dlist[i]<=t<=dlist[i+1] and \
                t+(1/(k*(M-n+0.000001)))*mp.log(1/p)>=dlist[i+1]:
                    time.append(dlist[i+1])
                    zz=np.random.binomial(n, pr, size=None)
                    burstt.append(zz)
                    n=n-zz
                    t=dlist[i+1]+0.0001
                    time.append(t)
                    break
            x=x+1
        g=g+1
    burst.append(burstt)
```

References

[1] J. S. Dittman, A. C. Kreitzer, and W. G. Regehr, "Interplay between facilitation, depression, and residual calcium at three presynaptic terminals," *Journal of Neuroscience*, vol. 20, no. 4, pp. 1374–1385, 2000.